



University of Tennessee, Knoxville
**Trace: Tennessee Research and Creative
Exchange**

University of Tennessee Honors Thesis Projects

University of Tennessee Honors Program

Spring 5-2002

Hybrid Fuel Cell/Gas Turbine Power Plant

James Bradley Alsup

University of Tennessee - Knoxville

Follow this and additional works at: https://trace.tennessee.edu/utk_chanhonoproj

Recommended Citation

Alsup, James Bradley, "Hybrid Fuel Cell/Gas Turbine Power Plant" (2002). *University of Tennessee Honors Thesis Projects*.
https://trace.tennessee.edu/utk_chanhonoproj/509

This is brought to you for free and open access by the University of Tennessee Honors Program at Trace: Tennessee Research and Creative Exchange. It has been accepted for inclusion in University of Tennessee Honors Thesis Projects by an authorized administrator of Trace: Tennessee Research and Creative Exchange. For more information, please contact trace@utk.edu.

UNIVERSITY HONORS PROGRAM

SENIOR PROJECT - APPROVAL


Name: Brad Alsop

College: Engineering Department: Mechanical (MABE)

Faculty Mentor: Dr. Fred Gilliam

PROJECT TITLE: Hybrid Fuel Cell / Gas Turbine Power Plant

I have reviewed this completed senior honors thesis with this student and certify that it is a project commensurate with honors level undergraduate research in this field.

Signed:  , Faculty Mentor

Date: 5-6-03

Comments (Optional):

Hybrid Fuel Cell Gas Turbine Power Plant

Submitted to: Dr. R.J. Krane

May 7, 2002

Brad Alsup

Jennifer Eckroth

Charles Freeman

Eric Lian

Marques Young

ME 479 Senior Design Team 3, Spring 2002

Executive Summary

Problem

Design a hybrid gas turbine/ solid oxide fuel cell power production system based upon the Siemens-Westinghouse model. The plant is to provide between three and five megawatts of power, which will be its base load. The plant is to use natural gas as its source of fuel. The customers who originated this project are three industrial plants whose operations are related. They are located in the same industrial park complex in Knoxville, TN. This plant will serve only their power needs, so there is no need to hook to the electrical grid. This project is to serve as a small-scale model for possible full-scale implementation in the future if it is effective from both a performance and a financial standpoint. Since that is the case, the economic feasibility of the plant must be analyzed using a present worth model.

Results

A system was designed that met the above specification. Specifically, a hybrid power system was designed that produced a base load of 4.3795 MW. The solid oxide fuel cell system produced 2.7515 MW while the gas turbine (EGT Hurricane) produced 1.628 MW. The model for the system was done using a FORTRAN code. This code generated all of the important parameters such as fuel and air flowrates, recuperator size, temperature values, size of the fuel cell generator system, and power outputs. All of these numbers are listed within the following report.

The hybrid system required a total flowrate of 37.79 kmol CH₄/h. This corresponds to a mass flowrate 606.20 kg/hr. Using this number, the system power output, and the LHV of methane (802,160 kJ/kmol), the overall system efficiency was found to be 52%. This value of efficiency is approximately equal to that which others have found in performing such studies.

A present worth study was performed on this project to determine its economic feasibility. The total cost of electricity of this plant is \$0.163/kWh. This economic analysis revealed that the plant would save a total of \$2,289,473.48 over the cost of buying electricity from the local utility provider during its thirty-year life span. Thus, the project will meet both its performance needs and its economic goal of saving the customer money.

Conclusions

While the design met the requirements established by the customer, many assumptions were made in the modeling of the power system. It would be the recommendation of this design team that the customer make a capital investment in research in the area of hybrid power systems while relying on traditional methods of power supply for the industrial facility. Should the project be eligible for a large government subsidy, it may become more feasible to pursue a quicker start up date. Since this design is modeled assuming “mature” technology, the current state of the fuel cell market and expense makes this power supply a less promising option. Without a grant or lowered fuel cell prices, it would not be a wise course of action for them to pursue this project at this time.

This design provides a platform for basic understanding of both gas turbine and fuel cell modeling. The information confirms research that has already been done in this area and does not charter any new thoughts in TSOFC or gas turbine research. A more in-depth study of the effects of pressure on the efficiency of fuel cells and a cost analysis on the system, matching power outputs and major components would be natural avenues for continued research as next steps.

Table of Contents

Executive Summary	i
Problem	i
Results.....	i
Conclusions	ii
Table of Contents	iii
Table of Figures	iv
Table of Tables	v
Nomenclature	1
Introduction	5
Background	5
Objective.....	6
Procedure	7
System Overview	9
Design and Analysis.....	11
Gas Turbine	11
Background	11
Gas Turbine Code Modeling	13
Fuel Cell	18
General Fuel Cell Background.....	18
Classifications of the SOFC	21
Combustion Preheater	32
Assumptions	35
Modeling the TSOFC	35
Analysis	38
Recuperator	40
Background.....	40
Recuperator Model.....	42
Other Plant Equipment.....	45
Fuel Processing System	45
Nitrogen Supply Systems.....	46
Startup Boiler	46
Auxiliary Air Compressor.....	46
Power Conditioning Unit.....	46
Economic Study	49
Environmental Impacts.....	58
Conclusion and Recommendations.....	60
Bibliography	61
Appendix	63
Appendix A.....	64
Appendix B.....	84
Appendix C	85

Table of Figures

Figure 1: Hybrid SOFC/ Gas Turbine power system	5
Figure 2: Complete system diagram.....	10
Figure 3: Temperature and pressure points for gas turbine system.	14
Figure 4: Individual fuel cell.....	18
Figure 5: Simplified fuel cell schematic	19
Figure 6: Tubular and planar solid oxide fuel cells	22
Figure 7: Exploded view of a TSOFC	23
Figure 8: Basic inputs and outputs to the TSOFC	24
Figure 9: Schematic of anode and cathode in TSOFC.....	25
Figure 10: Cell current vs. operating pressure	29
Figure 11: Predicted cell current vs. Cell voltage for TSOFC	30
Figure 12: Fuel cell thermal sources and sinks	33
Figure 13: TSOFC process flow in hybrid system	36
Figure 14: Heat exchanger in a recuperator.....	40
Figure 15: Crossflow recuperator	41
Figure 16: Temperature profiles for flow in a crossflow heat exchanger	42
Figure 17: Air quality index of Knxoville between May and September.....	58

Table of Tables

Table 1: European Gas Turbine (EGT) performance data 17
Table 2: Current from Hayness' pressure/ voltage chart 29
Table 3: Results from fuel cell code 39
Table 4: Capital cost estimates for a 4.3795 ME hybrid system..... 52
Table 5: Yearly COE associated with plant operation and upkeep..... 55

Nomenclature

Variable Name	Fortran Denotation	Definition	Units
c_{p,CO_2}	CPCO2	Constant pressure specific heat for CO ₂ of fuel cell exhaust gas	kJ/(kg-K)
c_{p,H_2O}	CPH2O	Constant pressure specific heat for H ₂ O of fuel cell exhaust gas	kJ/(kg-K)
c_{p,N_2}	CPN2	Constant pressure specific heat for N ₂ of fuel cell exhaust gas	kJ/(kg-K)
c_{p,O_2}	CPO2	Constant pressure specific heat for O ₂ of fuel cell exhaust gas	kJ/(kg-K)
ΔH_{CH_4}	DHCH4	Change in enthalpy—CH ₄	kJ/kmol
ΔH_{CO_2}	DHCO2	Change in enthalpy—CO ₂	kJ/kmol
ΔH_{H_2O}	DHH2O	Change in enthalpy—H ₂ O	kJ/kmol
ΔH_{N_2}	DHN2	Change in enthalpy—N ₂	kJ/kmol
ΔH_{O_2}	DHO2	Change in enthalpy—O ₂	kJ/kmol
$\dot{m}_{a,i}$	EMA	Initial estimate of mass flowrate of air	lb _m /s
\dot{m}_a / \dot{m}_F	EMAOMF	Ratio of mass flowrate of air to mass flowrate of fuel	lb _{ma} /lb _{mf}
\dot{m}_{EXCO_2}	EMCO2EX	Mass flowrate of exhaust CO ₂ (through HEX, muffler, and stack)	kg/h
$\dot{m}_{air,comp}$	EMCOMPAIR	Mass flowrate of compressor air	kg/s
\dot{m}_{EXGAS}	EMEXGAS	Mass flowrate of exhaust gas components (through HEX, muffler, and stack)	kg/h
\dot{m}_F	EMF	Mass flowrate of fuel for gas turbine	lb _m /s
\dot{m}_{EXH_2O}	EMH2OEX	Mass flowrate of exhaust H ₂ O (through HEX, muffler, and stack)	kg/h
$\dot{m}_{N_2,comp}$	EMN2COMP	Mass flowrate of N ₂ through compressor	kg/s
\dot{m}_{EXN_2}	EMN2EX	Mass flowrate of exhaust N ₂ (through HEX, muffler, and stack)	kg/h

Variable Name	Fortran Denotation	Definition	Units
$\dot{m}_{O_2,comp}$	EMO2COMP	Mass flowrate of O ₂ through compressor	kg/s
\dot{m}_{EXO_2}	EMO2EX	Mass flowrate of exhaust O ₂ (through HEX, muffler, and stack)	kg/h
\dot{n}_a / \dot{n}_F	ENAONF	Ratio of molar flowrate of air to molar flowrate of fuel	kmol _a /kmol _f
$\dot{n}_{CH_4,cell}$	ENCH4CELL	Total molar flowrate of methane per fuel cell	kmol _{CH4} /h
$\dot{n}_{CH_4,total}$	ENCH4TOTAL	Total molar flowrate of methane for entire system	kmol _{CH4} /h
$\dot{n}_{CO_2,6}$	ENCO26	Molar flowrate of CO ₂ at cell inlet	kmol/h
$\dot{n}_{CO_2,7}$	ENCO27	Molar flowrate of CO ₂ at cell outlet	kmol/h
\dot{n}_F	ENF	Molar flowrate of fuel for gas turbine	kmol/s
$\dot{n}_{H_2O,6}$	ENH2O6	Molar flowrate of H ₂ O at cell inlet	kmol/h
$\dot{n}_{H_2O,7}$	ENH2O7	Molar flowrate of H ₂ O at cell outlet	kmol/h
$\dot{n}_{N_2,6}$	ENN26	Molar flowrate of N ₂ at cell inlet	kmol/h
$\dot{n}_{N_2,7}$	ENN27	Molar flowrate of N ₂ at cell outlet	kmol/h
$\dot{n}_{O_2,6}$	ENO26	Molar flowrate of O ₂ at cell inlet	kmol/h
$\dot{n}_{O_2,7}$	ENO27	Molar flowrate of O ₂ at cell outlet	kmol/h
$(\dot{n}_{O_2,i}) / (\dot{n}_F)$	ENO2ONF	Ratio of molar flowrate of O ₂ at compressor inlet to molar flowrate of fuel	--
$\dot{n}_{oxstr,cell}$	ENOXSTRCELL	Molar flowrate of oxidizer stream per cell	kmol _{OXSTR} /h
$H_{f,0,CH_4}$	HF0CH4	Heat of formation of CH ₄	kJ/kmol
$H_{f,0,CO_2}$	HF0CO2	Heat of formation of CO ₂	kJ/kmol
$H_{f,0,H_2O}$	HF0H2O	Heat of formation of H ₂ O	kJ/kmol
$\Sigma \Delta p_0 / p_0$	SUMDELPOP	Sum of normalized total pressure losses in burner	
\dot{W}_C	WDOTC	Compressor power	kW
\dot{W}_E	WDOTE	Expander power	kW

Variable Name	Fortran Denotation	Definition	Units
\dot{W}_{EL}	WDOTEL	Electrical output of gas turbine under ISO conditions	kW
\dot{W}_{gen}	WGEN	Generator output	kW
--	ENCELL	Total number of fuel cells required	--
ϵ	EPSILON	Heat exchanger effectiveness	--
Φ_1	PHI1	--	--
Φ_2	PHI2	--	--
η_{CP}	ETACP	Compressor efficiency	--
η_E	ETAEP	Expander efficiency	--
η_{GB}	ETAGB	Gearbox efficiency	--
η_{GEN}	ETAGEN	Generator efficiency	--
ϵ_{ML}	EPSML	Factor to account for mechanical losses and windage	--
A_{HEX}	AHEX	Estimate of heat exchanger area	m ²
C	CRAT	Thermal capacity rate ratio for the HEX	--
C_c	CC	Thermal capacity rate of compressor stream	kJ/(h-K)
C_h	CH	Thermal capacity rate of exhaust gas stream	kJ/(h-K)
C_{max}	CMAX	Maximum thermal capacity rate for HEX	kJ/(h-K)
C_{min}	CMIN	Minimum thermal capacity rate for HEX	kJ/(h-K)
$c_{p,a}$	CPAAVE	Constant pressure specific heat of air	kJ/(kmol-K)
$c_{p,e}$	CPEAVE	Constant pressure specific heat of combustion products in expander	kJ/(kmol-K)
$c_{p,exgas}$	CPEXGAS	Constant pressure specific heat of exhaust gas	kJ/(kg-K)
HR	HR	Heat rate for gas turbine	Btu/(kW-h)
I_1	EYE1	Fuel cell data curve fit for V1=0.6V	A
I_2	EYE2	Fuel cell data curve fit for V2=0.75V	A

Variable Name	Fortran Denotation	Definition	Units
I_{cell}	EYECCELL	Cell current	A
NTU	ENTU	Load data for heat exchanger	--
p_{06}	P06	Pressure drop of exhaust gases in SOFC	atm
p_{07}	P07	Pressure drop of exhaust gases in stack	atm
p_{08}	P08	Pressure drop in muffler and stack	atm
p_{cell}	CELLPRESS	Fuel cell operating pressure	atm
P_{cell}	PCELL	Actual cell power	W
$P_{tot,fc}$	TOTPOWFC	Total power to be generated by fuel cells in plant	MW
Q_{HEX}	QHEX	Rate of heat transfer to cold stream in HEX	kJ/h
R_c	RC	Compressor pressure ratio	--
R_E	RE	Expander pressure ratio	--
T_{01}	T01	Atmospheric temperature	K
T_{02}	T02	Compressor outlet temperature	K
T_{02I}	T02I	Initial estimate of compressor outlet temperature	K
T_{03}	T03	Outlet temperature of the compressor air stream	K
T_{03I}	T03I	Initial estimate of compressor air heat exchanger outlet temperature	K
T_{041}	T041	Turbine inlet temperature	K
T_{05}	T05	Expander outlet temperature	K
T_{05I}	T05I	Initial estimate of expander outlet temperature	K
T_{06}	T06	Initial estimate of oxidizer stream inlet temperature	K
T_{08}	T08	Outlet temperature of exhaust gas stream	K
U	U	Overall heat transfer coefficient	kJ/(h-K-m ²)
U_F	UF	Fuel utilization factor	--
V_{CELL}	VCELL	Cell operating voltage	V

Introduction

Background

The ever growing need for electrical power around the world coupled with a shrinking supply of fossil fuels has made finding alternative methods of generating power increasingly more important. Research is being conducted on many different forms of power production, such as wind power, solar power, and new forms of nuclear power, at a furious rate in hopes of finding the energy source of tomorrow. While much of this research is promising, none of these alternatives have yet reached the stage where they are feasible and/or accepted by the general public as legitimate for power production. Thus, something must be done using existing technology to satiate the desire for power while conserving the limited supply of natural resources that are available through increased efficiency. One of the strongest candidates for new power production systems is a hybrid system that combines a gas turbine with a solid oxide fuel cell (SOFC). A very basic diagram of this hybrid system can be seen below in Figure 1.

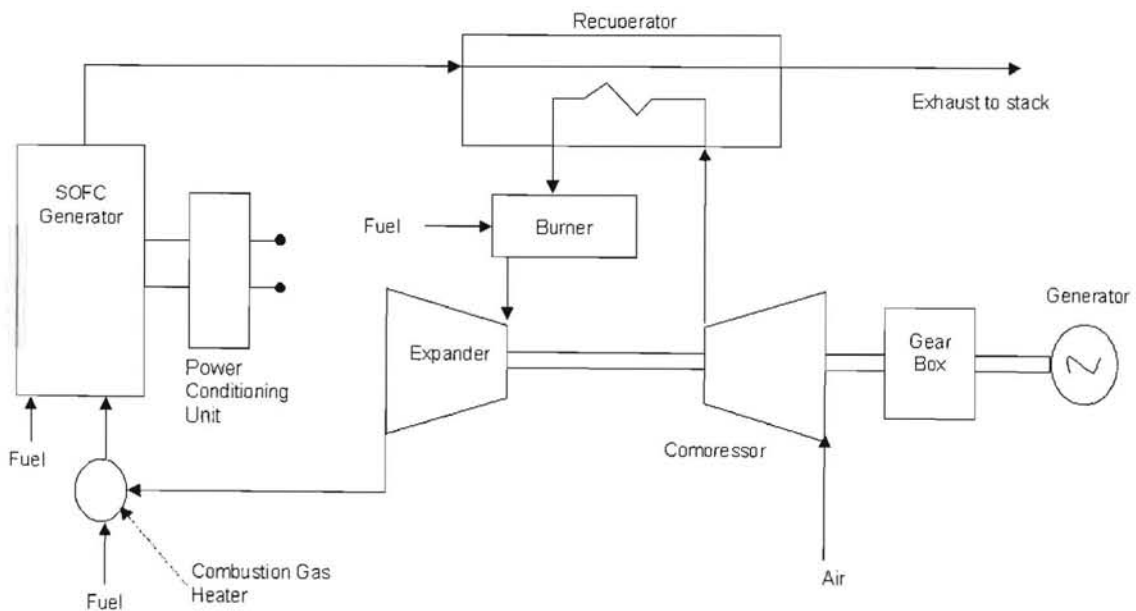


Figure 1: Hybrid SOFC/ Gas Turbine power system

As can be seen in Figure 1, such a plant is regenerative in that it uses the exhaust gases from the gas turbine expander to provide the SOFC with the oxygen required for the electrochemical reactions that take place therein. Furthermore, the hot exhaust gases leaving the SOFC are used to heat the air for the gas turbine after it leaves the compressor stage and before it enters the burner. These features have the effect of driving the efficiency of the system up and decreasing the amount of fuel necessary to perform the intended tasks. Due to these very desirable attributes, the hybrid SOFC/ gas turbine power system is one that is gaining much attention, especially from the Department of Energy (DOE), which hopes plants utilizing pressurized systems and operating at seventy percent efficiency will be in operation by the year 2010 with plants operating at eighty percent efficiency up and running by 2015. In preliminary field tests, these systems, which utilized tubular solid oxide fuel cells (TSOFC) and micro gas turbines, were both extremely efficient (though they have yet to reach the above target values) and reliable, running for several thousand hours nonstop. It should be noted that atmospheric systems cannot attain an operating efficiency as high as 70% at this time, but they are capable of efficiencies above 50%. Thus, this type of system will be a great improvement over many of the current power production systems.

In addition to the high efficiencies and great reliability, hybrid power systems can be made in almost any size range. The first prototypes generated less than 100 kW of power, but it is possible to build plants that will produce many megawatts. This versatility is due to the wide range of gas turbine sizes available as well as to the ability that exists to stack fuel cells to produce more and more power. The possibility of achieving almost any level of power production, along with high efficiencies and reliable service, makes hybrid systems very attractive alternatives to the coal-fired plants and traditional nuclear reactors that are in service today.

Objective

Because the power system described above is so promising, and so versatile, many industrial plants or groups of industrial plants located in the same area might wish to build one that will serve its/their power demands. Doing so could possibly have

the effect of lowering their power bills since they would no longer be buying electricity from a local utility. The purpose of this study is to assess just such a situation. The customer would like to construct a pilot system using the technology just discussed that would serve as a test case, and possible model, for full-scale implementation of such power systems into its business practice.

Specifically, the customers, three plants located within the same industrial park, want to build a small system, on the scale of 3.5-5 MW, in Knoxville, TN. This system is to use natural gas as a fuel and will operate at atmospheric pressure. The plant will be base-loaded and changes in power demands need not be considered. It should be modeled on the system already designed by Siemens-Westinghouse Corporation. As part of the design process, the economic feasibility of the plant must be assessed in order to determine whether or not the investment is a wise one for the company to make. This decision will be based upon a present worth study of the yearly costs and revenues over the life of the plant. The customer has specified that the minimum attractive rate of return (MARR), or hurdle rate, for such a project will be sixteen percent.

Procedure

In order to fulfill the customer's needs and meet all specified operating conditions, a careful model of the system had to be built. To accomplish this, a Fortran code was written that followed the Siemens-Westinghouse model fairly closely. This code, and thus the model utilized in this study, was simplified quite a bit, but it still retains its accuracy in predicting the performance of the hybrid system. The assumptions that were made to achieve this simplification were all well justified and will be explained in latter sections of this report.

Before the system could be modeled, however, several decisions had to be made about the operation characteristics of the system. First, a base-load had to be defined. It was decided that the customer needs a system that is capable of producing 4.3795 MW of power. Next, the amount of the total power generated by each section of the system had to be determined. To do this, a gas turbine with a

known power output was chosen. Fuel cell stacks were then used to produce the remainder of the required power. In choosing the total power output of the fuel cell stacks, the size of the units produced by Siemens-Westinghouse had to be taken into consideration. One fuel cell module contains 11,520 cells. Thus, a value for the fuel cell power output had to be chosen that would allow for a multiple of this number to be used. Doing so would help to facilitate the purchase of the TSOFC generator from Siemens-Westinghouse.

Once these parameters, as well as other pertinent operating conditions such as the local atmospheric temperature and pressure, were found, the model could be built. All the necessary operating conditions and given performance data were entered into the code, which generated values for the unknowns of the system, such as required flowrates of fuel and air and the exit temperature of all air flows. Finally, the information that the model yielded was used in a present worth study to determine whether or not building such a power system was a sound decision from an economic standpoint.

System Overview

The hybrid gas turbine/ solid oxide fuel cell power system that was designed in this project utilized two very promising power production technologies in tandem to create a very efficient system of making electricity. The gas turbine side of the plant burns natural gas with air in a combustion chamber. The products of this combustion reaction then go through an expander, which turns a shaft. The shaft does two things. First, it provides power to a compressor that brings in the air necessary for the combustion reaction. Second, it turns a generator that produces electricity. As air is taken from the atmosphere and is compressed, it runs through a recuperative heat exchanger where it is heated before entering the combustion chamber. This preheating operation helps to increase the efficiency of the system while lowering the amount of fuel that must be burned in the combustion chamber.

Once the air leaves the expander, it flows to the solid oxide fuel cell system, where it will perform its role as an oxidizing agent. Before this air enters the SOFC, it is preheated in a second combustion chamber to increase its temperature to the target operating temperature of the fuel cell. In the fuel cell system, both chemical and electrochemical reactions take place to turn the chemical energy stored within the natural gas fuel into electrical energy. This energy is initially in the form of direct current but is converted to alternating current by a power-conditioning unit. The extremely hot exhaust gases that leave the fuel cell system are pumped to the recuperator where they provide the heat that is necessary to raise the temperature of compressed air before it enters the combustion chamber. This regenerative feature makes the power system described above more efficient and cost effective. A process flow diagram of the system can be found in Figure 2 below.

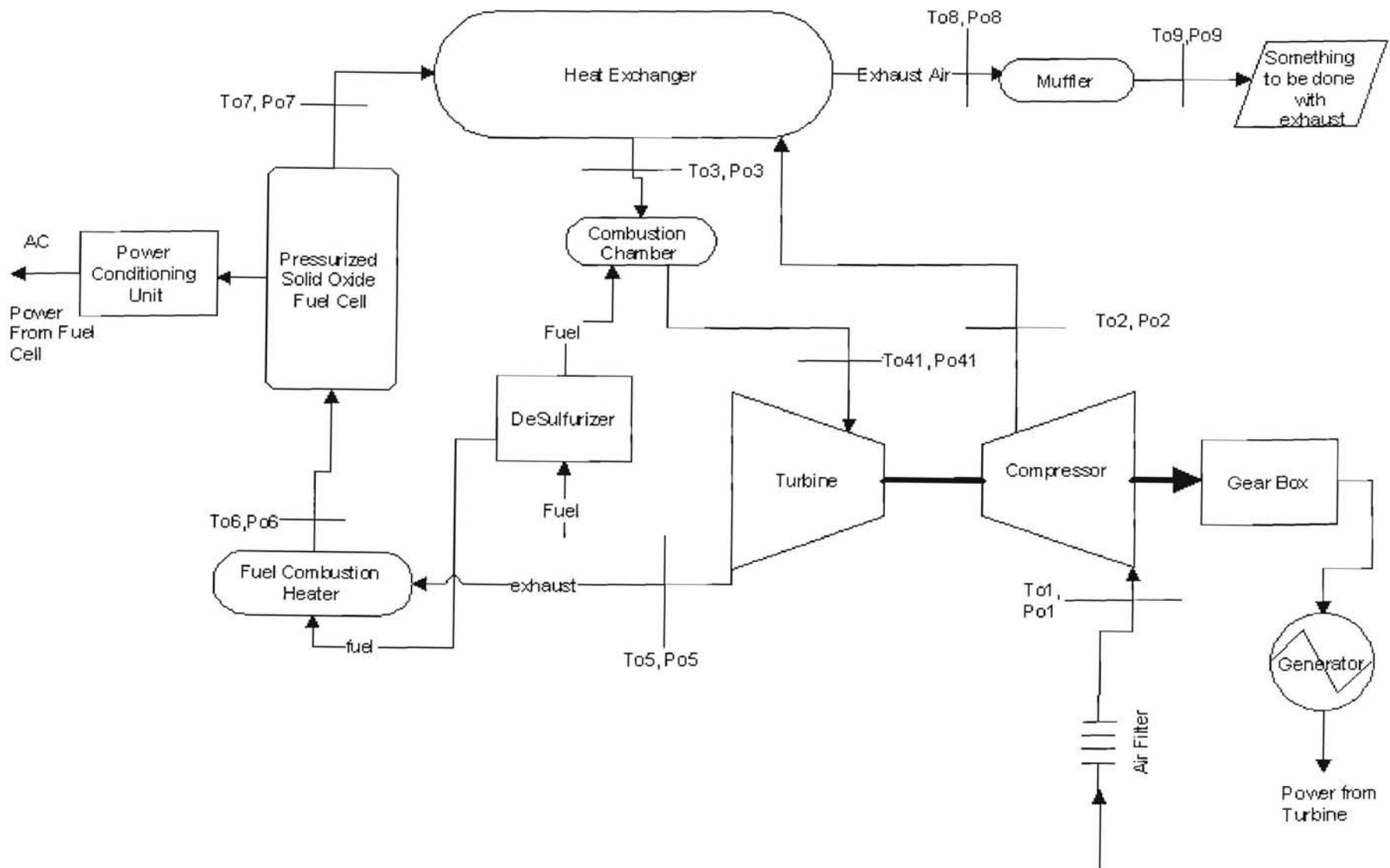


Figure 2: Complete system diagram

Design and Analysis

Gas Turbine

Background

A turbomachine is a device that (1) produces a change in enthalpy in a stream of fluid passing through it and (2) transfers work through a rotating shaft. Work is performed in a turbomachine by the flowing fluid exerting forces on the blades rigidly attached to the rotating shaft.

A gas turbine is a turbomachine that either (1) produces a net shaft work output, or (2) produces a high pressure and temperature stream of gas that is expanded through a nozzle to produce thrust. All gas turbines are heat engines, and most gas turbines are internal combustion engines. The gas turbine of present interest operates on an “open cycle” and is a simple cycle, single-shaft turbine consisting of a compressor, combustion chamber (or burner), a turbine (or expander), and an electrical generator.

A “modified” calorically perfect ideal gas model is used, meaning constant specific heats, c_p and c_v , with suitably averaged values.

$$\bar{C}_p = \frac{\int_{T_1}^{T_2} C_p(T) dT}{T_2 - T_1} \approx \frac{C_p(T_1) + C_p(T_2)}{2} \quad (1)$$

$$\bar{C}_v = \frac{\int_{T_1}^{T_2} C_v(T) dT}{T_2 - T_1} \approx \frac{C_v(T_1) + C_v(T_2)}{2} \quad (2)$$

$$\text{For an ideal gas: } \bar{C}_p - \bar{C}_v = R \quad (3)$$

$$T ds = dh - v dP$$

$$ds = \frac{dh}{T} - \frac{v}{T} dP$$

$$\text{For an ideal gas: } dh = \bar{C}_p dT \text{ and } \frac{v}{T} = \frac{R}{P}$$

$$\text{substituting gives: } \int_1^2 ds = \bar{C}_p \int_{T_1}^{T_2} \frac{dT}{T} - R \int_{P_1}^{P_2} \frac{dP}{P}$$

$$s_2 - s_1 = \bar{C}_p \ln\left(\frac{T_2}{T_1}\right) - R \ln\left(\frac{P_2}{P_1}\right) \quad (4)$$

If two states of a flowing fluid are connected by an isentropic process, $s_1 = s_2$, Equation (4) gives:

$$0 = \bar{C}_p \ln\left(\frac{T_2}{T_1}\right) - R \ln\left(\frac{P_2}{P_1}\right)$$

$$\ln\left(\frac{T_2}{T_1}\right) = \frac{R}{\bar{C}_p} \ln\left(\frac{P_2}{P_1}\right) = \ln\left(\frac{P_2}{P_1}\right)^{\bar{R}/\bar{C}_p}$$

$$\frac{T_2}{T_1} = \left(\frac{P_2}{P_1}\right)^{\bar{R}/\bar{C}_p}$$

Turbomachinery efficiency compares actual work transfer with the work transfer in an idealized process. The ideal process is polytropic for this model. The inlet and outlet planes are identified for all analyzed elements within the model, the outlet stagnation pressure is the actual stagnation pressure, which is the static pressure or atmospheric pressure, and the actual work includes losses from the bearings and friction. Polytropic ("small-stage) efficiency removes the effect of pressure ratio and enables valid comparisons between machines with different pressure ratios. Therefore, analysis of gas turbine cycles are simplified because a single value of polytropic efficiency may be used for each compression and expansion process instead of isentropic efficiencies that depend on pressure ratio. According to Korakianitus and Wilson ¹, the polytropic efficiencies for the compressor and expander for simple gas turbine models are given below, with both being polytropic stagnation-to-stagnation efficiencies.

¹ Korakianitus 381-388.

$$\zeta_{c, p} = 0.91 - \frac{r_c - 1}{300} \quad (\text{Compressor efficiency})$$

$$\zeta_{t, p} = 0.90 - \frac{r_t - 1}{250} \quad (\text{Expander efficiency})$$

Comparing the magnitudes of pressure ratios within the gas turbine, the combustion process has the largest pressure loss of any process in a gas turbine. The exhaust speed from the compressor is on the order of 125-200 m/s. A flame speed of approximately 10 m/s is attainable for the maximum fuel-to-air ratio. Therefore, the fluid leaving the compressor must be retarded; this deceleration is achieved inefficiently by putting the fluid through a diffuser (baffles) to recover some of the kinetic energy and static pressure. Without this deceleration of the compressor exhaust, the flame will be blown out of the burner, and complete combustion of the fuel within the burner will not occur. As a result, there is a fairly high and unavoidable viscous pressure loss in the combustion process of approximately 4-5% of the burner inlet pressure.

Assumptions

Several assumptions are made throughout the analysis of the simple-cycle gas turbine engine to simplify complex calculations necessary for appropriate evaluation of the gas turbine engine performance. Perhaps, the key assumption made in the analysis is that the combustion reaction within the combustion chamber goes to completion, or one hundred percent of the fuel is burned. Also, modeling is based on the utilization of pure methane (CH_4) as a fuel source. Although the natural gas content in the Knoxville area is approximately 97% CH_4 , this minor discrepancy between actual and theoretical fuel composition will create uncertainty in the performance data, but not enough to misrepresent the true performance of the engine.

Gas Turbine Code Modeling

A pressurized hybrid SOFC/GT power generation system, base-loaded with natural gas as the fuel, is desired. The rated capacity for the system must fall between 3 MW and 5 MW. The GT utilized must be a simple-cycle, single-shaft

engine that meets the power output requirements. After reviewing several engines that met these constraints, the European Gas Turbines (EGT) Hurricane engine was selected. This selection was made for a variety of reasons, but the two most prevalent were the engine's power rating and expander outlet temperature. An exit temperature as high as possible was desired in order to decrease the amount of air preheating that would have to be done on the traveling from the gas turbine to the SOFC generator. Once the engine to be used was selected, a computer performance model of the system was built using a FORTRAN code. This code can be found in Appendix A. Figure 3 below lists all of the temperature and pressure points of import for the gas turbine model. The FORTRAN code references this information in its calculations.

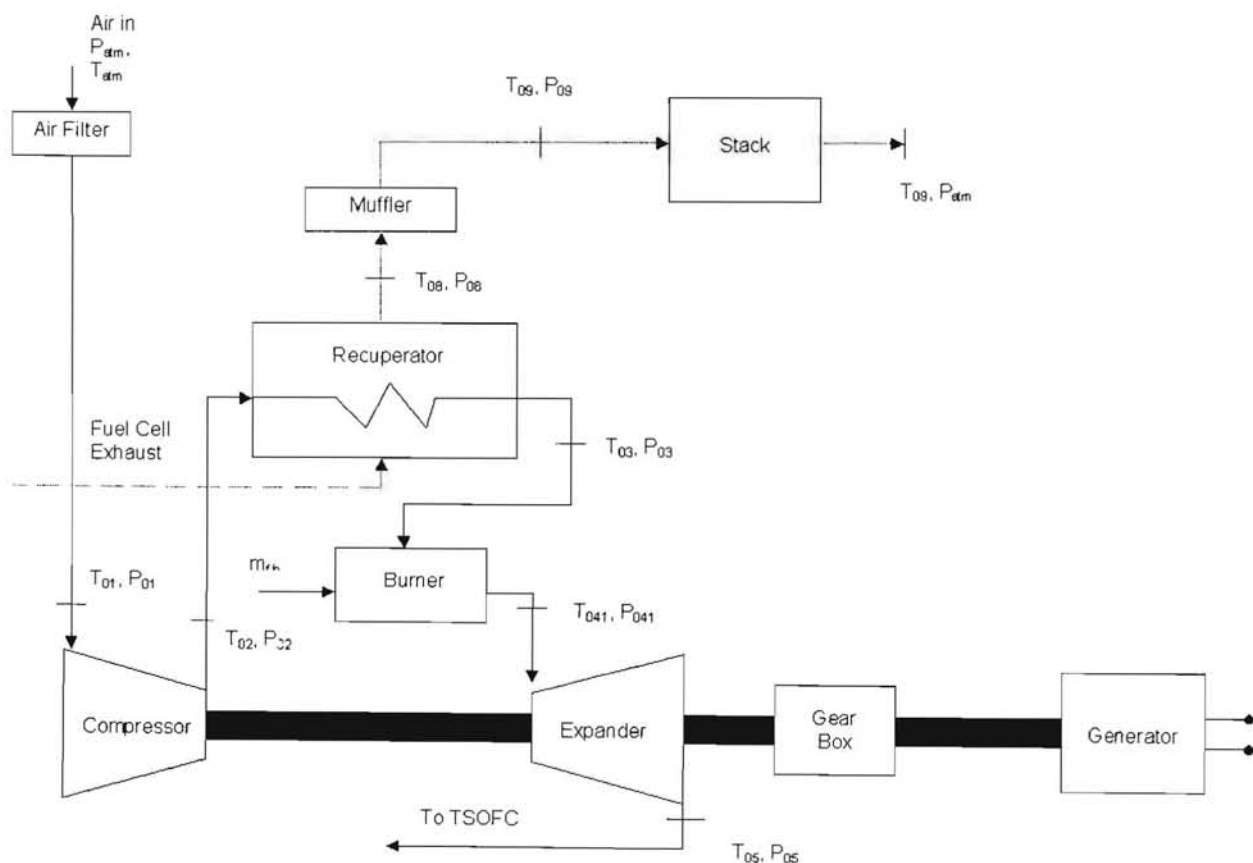


Figure 3: Temperature and pressure points for gas turbine system.

Enthalpy change calculations used for input into the FORTRAN code were derived from Scott and R.E. Sonntag² for the GT combustion model. Enthalpy changes for CH₄, O₂, N₂, H₂O, and CO₂ were calculated over the entire GT cycle for comprehensive analysis. For the accompanying FORTRAN code, the following parameters are known and given as user-inputs:

Nomenclature: Temperature variables correlate to the GT schematic.

RC = compressor pressure ratio

T01 = ambient temperature and compressor inlet temperature, [K]

T041= turbine inlet temperature, [K]

SUMDELPOP = $\Sigma(\Delta P/P_o)$ = sum of the normalized total pressure losses

EMA = initial estimate of mass flow rate of air, [lbm/s]

ETAGEN = generator efficiency

ETAGB = gearbox efficiency

ETACP = compressor efficiency

ETAEP = expander efficiency

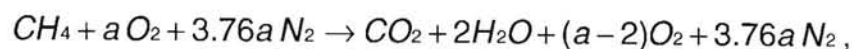
ESPML = mechanical losses and “windage”

WDOTEL = electrical power output of the turbine under ISO conditions, [kW]

T03I = initial estimate of compressor air heat exchanger outlet temperature, [K]

T05I = initial estimate of the expander outlet temperature, [K]

After the user has input all of the known components of the GT, the code processes through an iterative loop to calculate the compressor outlet temperature, *T02*. Another series of enthalpy change calculations are performed on the burner to calculate the overall combustion equation



² Scott p. 113.

where a is given to be the molar air-to-fuel ratio, $\frac{\dot{n}_{O_2,i}}{\dot{n}_F} = \frac{\Phi_1}{\Phi_2}$, denoted as

ENO2ONF in the FORTRAN code. An initial guess is input by the user for the expander outlet temperature, *T05I*, with a subsequent calculation of the correct expander outlet temperature, *T05*, using another iterative loop. The average molar constant pressure specific heat of the combustion products in the expander, *CPEAVE*, is the driving force in determining the correct expander outlet temperature. Once the expander outlet temperature has been determined, the FORTRAN code then computes the following variables necessary for analysis of the GT engine:

ENAONF = air-to-fuel molar flow rate, [kmol air/kmol fuel]
EMAOMF = air-to-fuel mass flow rate, [kg air/kg fuel]
EMF = mass flow rate of fuel, [lbm/s]
ENF = molar flow rate of fuel, [kmol/s]
ENO2 = molar oxygen flow rate through the compressor, [kmol/s]
T02 = compressor outlet and burner inlet temperature, [K]
T05 = expander outlet temperature, [K]
WDOTC = compressor power, [kW]
WDOTE= expander power, [kW]
WDOTGEN= generator power, [kW]
HR = gas turbine heat rate, [Btu/(kW-hr)]

Table 1 below gives the input data and accompanying results for the EGT Hurricane GT engine as prescribed earlier to meet the design criterion specified by the client.

Table 1: European Gas Turbine (EGT) performance data

European Gas Turbines (EGT) Hurricane Gas Turbine Engine			
Input Data		Output Data	
T01 (K)	288	ENO2ONF	26.058
T041 (K)	1161	ENAONF (kmol_{air}/kmol_f)	124.036
SUMDELPOP	0.085	EMAOMF (kg_{air}/kg_f)	224.023
ETACP	0.85	ENF (kmol/s)	0.00279
ETAEP	0.86	EMF (lb_m/s)	0.09866
ETAGEN	0.97	CPAAVE (kJ/kmol-K)	29.681
ETAGB	0.975	CPEAVE_{ave} (kJ/kmol-K)	33.107
EPSML	0.02	ENO2 (kmol/s)	0.0727
T05I (K)	875	T02 (K)	598.41
EMA (lb_m/s)	16	T05 (K)	732.86
WDOTEL (kW)	1628	WDOTC (kW)	3188.5
R_c	9.2	WDOE (kW)	4945.0
		EMA (lb_m/s)	22.103
		WGEN (kW)	1628

In comparison to the performance information documented in the 1996-97 Gas Turbine World Performance Specs, the calculated performance of the European Hurricane Gas Turbine engine via the documented FORTRAN code gave fairly accurate results. The documented turbine inlet temperature of 2073°F (1407 K) was 2.49% greater than the turbine inlet temperature of 1327 K (1928.9°F) calculated by the code. The air mass flow rate was found to be 22.103 lbm/s, while the documented literature indicates an air mass flow rate of 16.3 lbm/s for the European Hurricane Gas Turbine. This large deviation between flow rates is due in part to the aforementioned assumptions regarding the amount of fuel reacted and burned within the combustor. Since it is assumed that the methane gas is burned to completion, less fuel flow is required to satisfy the needs of the turbine to achieve its nominal power output. Exhaust temperatures from the literature and the FORTRAN code are 875.37 K (1116°F) and 732.86 K (859.5°F), respectively. From the data obtained, the turbine performance exhibited from the Hybrid Gas Turbine/Solid Oxide Fuel Cell Power Generation System has a strong positive correlation to published performance data indicated by the manufacturer.

Fuel Cell

General Fuel Cell Background

Fuel cells are electrochemical devices that convert the chemical energy of a chemical reaction directly into electrical energy. They are often classified as batteries where the electrodes do not lose their power to convert electrons to current, but they must be continually supplied with fuel and oxygen. The basic structure of a fuel cell consists of an electrolyte layer in contact with a porous anode and cathode on either side as shown in Figure 4.

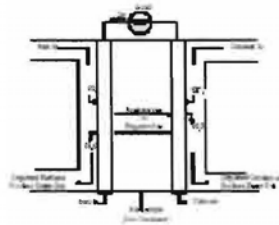


Figure 4: Individual fuel cell

As the oxygen passes through the cathode, the amount of oxygen in the mixture near the cathode surface is reduced. The size of this reduction depends on the fluid flow and mass transfer of the gas mixture near the cathode surface. The reduction of oxygen causes a reduction in partial pressure of oxygen near the surface, which in turn causes a reduction in the cell voltage.

Near the cathode surface oxygen is replenished by diffusion taking place with the incoming air. Similar reductions in the partial pressure of hydrogen can occur in the vicinity of the anode, which will also reduce cell voltage.

In either case, as the current increases if it is not held at a steady rate, the flow of oxygen or hydrogen cannot be replenished by mass diffusion at a sufficient rate to keep up with increasing demands of the cell half reactions. Below is a diagram in figure 5 of a simplified model of the flows through a fuel cell.

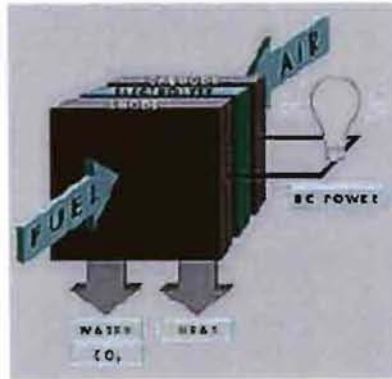


Figure 5: Simplified fuel cell schematic

Fuel cells have a wide variety of applications ranging from cell phones to automobiles to power plants for buildings. There is a wide variety of fuel cells available for these different applications. The major difference among the different types of fuel cells is the electrolyte that is utilized. A brief description of the various electrolyte cells from the Fuel Cell Handbook (fifth edition) issued by the U. S. Department of Energy is given below.

Polymer Electrolyte Fuel Cell (PEFC): The electrolyte in this fuel cell is an ion exchanger membrane that is an excellent conductor. Corrosion is kept to minimum in these cells because the only liquid in this fuel cell is water. The limiting factor in this design is that the temperature cannot be over 120°C so that the resulting water does not evaporate faster than it is produced. The water plays an integral role in hydrating the membrane.

Phosphoric Acid Fuel Cell (PAFC): Phosphoric acid concentrated to 100% is used for the electrolyte in this fuel cell, which operates at 150 to 220°C. The temperature range is important because at lower temperatures the acid is a poor conductor, and CO poisoning becomes severe. Phosphoric acid is relatively stable compared to other common acids. Because of this the PAFC is capable of operating at high temperatures (100 to 220°C). This cell also makes water management less difficult than some because the use of concentrated acid (100%) minimizes the water vapor pressure.

Molten Carbonate Fuel Cell (MCFC): The MCFC uses a molten carbonate salt mixture as its electrolyte. The composition of the electrolyte varies, but usually consists of lithium carbonate and potassium carbonate. At the operating temperature of about 1200°F (650°C), the salt mixture is liquid and a good conductor. Given the high temperatures and operating efficiencies, the MCFCs are the most common alternative to SOFC in high temperature applications.

Tubular Solid Oxide Fuel Cell (TSOFC): The electrolyte in this fuel cell is a solid, nonporous metal oxide, usually Y₂O₃-stabilized ZrO₂. The cell operates at 1000°C where ionic conduction by oxygen ions takes place. Typically, the anode is Co-ZrO₂ or Ni-ZrO₂ cermet, and the cathode is Sr-doped LaMnO₃.

Since each fuel cell type has a different method of operating, they are each suited for varying applications. The PEFC for example operates best at low temperatures, which means the cell can reach its operating temperature quickly. The AFC was one of the first fuel cells developed in modern times; its most notorious application was to provide power for the Apollo space vehicle. It was chosen for this application because of its performance with Hydrogen and Oxygen and its flexibility to use a wide range of electrocatalysts. A major disadvantage of this system was that even a small amount of CO₂ within the air would poison the system. When this was coupled with purification of the hydrogen, it was deemed not cost effective to pursue in commercial applications in the United States. The fuel cells that operate at higher temperatures, the MCFC and SOFC have advantages that cannot be met by the lower temperature systems. The cells can be made of materials that are easily fabricated like sheet metals in the case of MCFC or ceramics in SOFC. Carbon dioxide can be used a fuel as well as hydrogen and the heated exhaust is sufficiently high enough to drive a gas turbine and/or produce high pressure steam for use in a steam turbine. One of the most important advantages is that CO₂ reacts across the cathode to produce additional current

Solid Oxide Fuel Cell Background

Fuel Cells are commonly classified by the types of electrolyte they use and the temperatures at which they operate. The Solid Oxide Fuel Cell uses a solid ceramic electrolyte. This is a marked difference from other fuel cells that use a liquid electrolyte. At temperatures between 900 and 1000° C the mobility of the oxygen ions through the electrolyte is sufficient enough to conduct electrical current. A SOFC will not only convert H₂ to electricity, but also will efficiently convert CO into electricity and heat. Unlike other low temperature fuel cells in which the CO will act as poison to the catalyst even in PPM concentrations, the CO in a SOFC does not have to be removed. Instead of being a contaminant of the system, it can become a source for additional current.³

Because the SOFC does not use a liquid electrolyte, there is no inherent corrosion of the electrolyte material. Internal reforming is an important key benefit of the SOFC when operated at high temperatures. This is a significant advantage for SOFC since it eliminates the need for an external reformer to produce the hydrogen. Hydrogen is instead produced directly through the reforming process inside the cell. But for all of the benefits with using temperatures greater than 800° C, those same temperatures place stringent requirements on the materials that can be used in a SOFC. Developing low cost materials and the cost of the ceramic structures are key challenges facing SOFC technology.⁴

Classifications of the SOFC

There are two main types of competing technology in the SOFC market today, planar style and tubular style. One of the first major design decisions in this project was the consideration of the merits of each type of SOFC and the choice of one with which to continue.

Planar solid oxide fuel cells are being studied and produced by such notable companies as McDermott Technologies and Global Tech. Planar Fuel cells are hooked up with bi-polar interconnects. The advantages of this design are lower

³ Cirkel, p . 2

⁴ Fuel Cell handbook, p. 8-1.

ohmic losses, which result in somewhat higher efficiency and greater power density. The disadvantages are almost overwhelming. The most inherent problem with this technology is the propensity for the fuel cell to leak around the seals. Figure 6 below depicts each of the aforementioned types of fuel cell. Tubular Solid Oxide Fuel Cells TSOFC such as those being developed by Siemens Westinghouse are considered by many to be the most appropriate type to marry with gas turbines in power systems. The technology has been in development in various forms since the late 1950's. It is on tubular technology that this design is based.

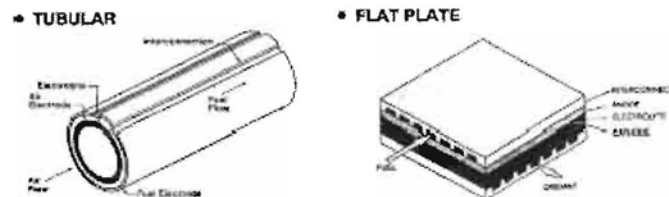


Figure 6: Tubular and planar solid oxide fuel cells

The standard Siemens Westinghouse tubular cell is 150cm long as seen in the following figure and is closed at one end. They are 2.2 cm in diameter and are bundled in groups of twenty-four cells or tubes into a stack. The diagram below, figure 7, shows the basic configuration. The figure shows a group of closed tubular cells composed of concentric electrodes and separated by the ceramic electrolyte. Fuel flows upward between the tube exteriors, while process air flows upwards in the annular space between the air feed tube and the cell inner surface. The contacts between cells are nickel felt contacts.

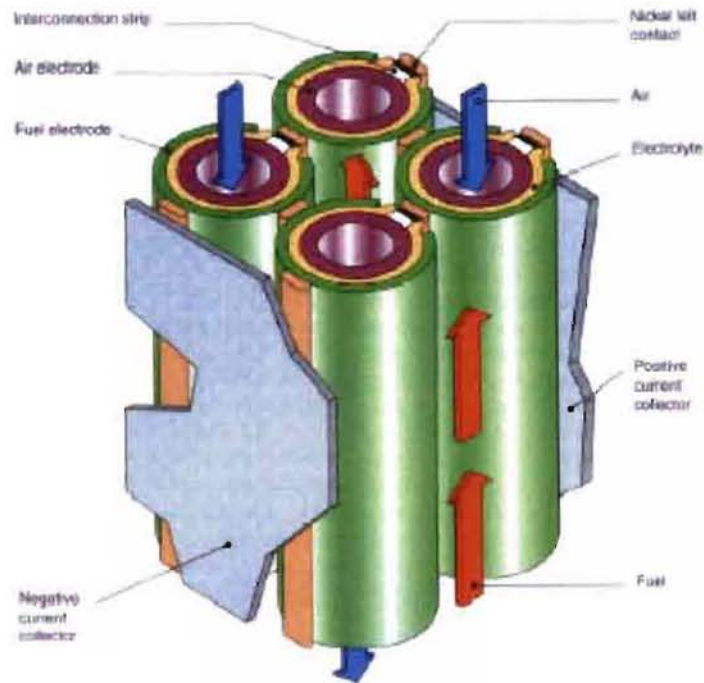


Figure 7: Exploded view of a TSOFC

Basic SOFC Calculations

In this design, material was available from which the design team was able to interpolate much of the key empirical data that would have been otherwise lengthy and difficult to ascertain. Before delving into the details of that interpolation, it was important to understand the fundamental equations and calculations that make up the basis for fuel cell modeling.

Figure 8 depicts the inputs and outputs of the fuel cell to better understand how it works. In simplistic terms hydrogen and oxygen are sources for energy entering the fuel cell and the overall products of the reactions inside the cell produce energy in the form of electricity and heat. The chemical reactions themselves produce water.

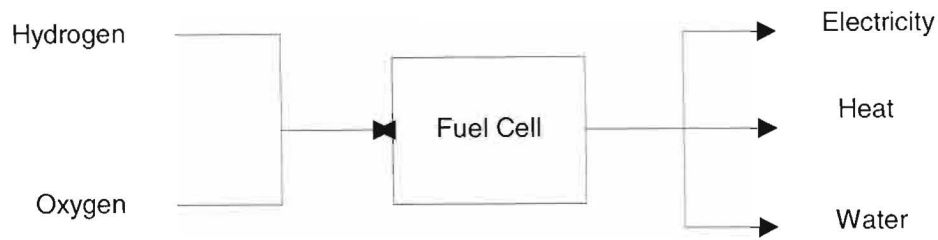
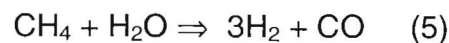


Figure 8: Basic inputs and outputs to the TSOFC

To determine values for the electrical power and energy, well-known formulas are available for simple calculations:

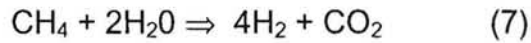
$$\text{Power} = VI \quad \text{and} \quad \text{Energy} = V/t$$

Understanding the chemical inputs and outputs is not as easily accomplished. There are two major types of reactions going on in the fuel cell. There are the chemical reactions and the electrochemical reactions. In this design, methane was chosen as the fuel or primary source of the hydrogen. Before the fuel is a useable source of hydrogen it must be reformed. As stated before, this is one of the key benefits of using a SOFC; the reforming can take place within the cell, eliminating the need for a reformer. The reforming reaction is represented below by equation (5):



A second chemical reaction, the water-gas shift reaction, also takes place within the cell. In it, the carbon monoxide from the reforming reactions reacts with water to create more hydrogen and carbon dioxide. This equation is shown below in equation (6).





In a fuel cell, the "external work" involves moving electrons round an external circuit. Any work done by a change in volume between the input and output is not harnessed. The Gibbs free energy is used to determine the energy available to do external work. It is the change of energy that is important. In a fuel cell, it is the change in the Gibbs free energy of formation, ΔG_f , that establishes the amount of energy that is released. The Gibbs free energy of formation is not constant but changes with temperature and state. If there are no losses in the fuel cell or if the process is reversible, then all this Gibbs free energy is converted into electrical energy. In reality, some of the energy is also released as heat.

The actual chemical reactions take place on the surface of the anode. But to understand the flow of the electrons to create current, it is the electrochemistry that must be understood. The diagram represented in Figure 9 below is a schematic of the anode and cathode.

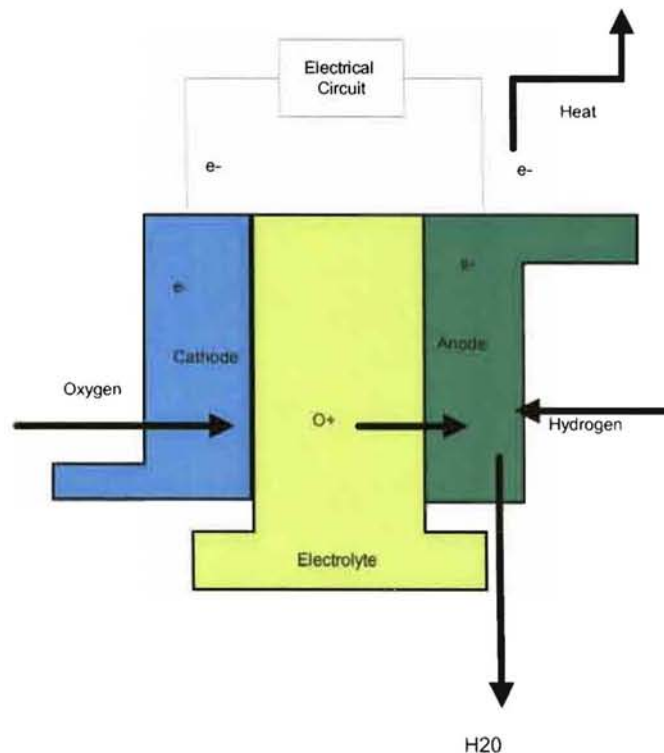
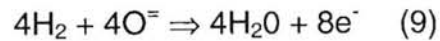


Figure 9: Schematic of anode and cathode in TSOFC

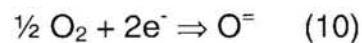
At the anode of the TSOFC, the electrochemical reaction takes place in the form of equation 8. It is at this point that the hydrogen is oxidized to form water.



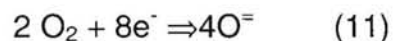
Since our overall chemical reaction created four hydrogen molecules, the actual reaction is shown in equation (9).



The electrochemical reaction at the cathode is the oxidizing reaction. It is here that reaction occurs to produce the oxygen ion used to produce water. The electrochemical reaction is shown in equation (10):



For the four moles of water created in the chemical reaction four oxygen ions are needed. Equation 11 represents this reaction.



It is from these reactions that the actual current created by the fuel cells can be established. The ideal performance of the cell can then be defined by its Nernst potential represented as cell voltage. The Nernst equation establishes a relationship between the ideal cell potential (E^0) for the cell reaction and the ideal equilibrium potential (E) at other partial pressures and temperatures. This equation is extremely important in understanding the output of the fuel cell because once the ideal potential at standard conditions is known, the ideal voltage can be determined at other temperatures and pressures. With this in mind, the Nernst equation can be used to determine that at higher reactant pressures, the ideal cell potential can be increased with a constant cell temperature. This has been the source of much study in the fuel cell community.

pressures, the ideal cell potential can be increased with a constant cell temperature. This has been the source of much study in the fuel cell community.

To get the ideal voltage, performance curves are necessary from the manufacturer. In the cutthroat world of SOFC research, this information is often proprietary and difficult to obtain. In this design project, initial fuel cell modeling was done using the fuel cell performance curves of the Siemens Westinghouse Tubular SOFC. The availability of this information was a key factor in choosing that product as the cornerstone for the fuel cell design.

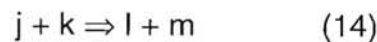
The Nernst equation for the fuel cell model is shown below in equation (12) where F is equal to Faraday's constant, which is the charge per mole of electron, N is equal to the number of electrons released in a mole of fuel.

$$E = E_0 + \frac{RT}{NF} \ln \left[\frac{P_{\text{reactants}}}{P_{\text{products}}} \right] \quad (12)$$

The Nernst equation establishes the relationships from the effects of changing pressure and gas concentration. For the cases of gases behaving like "ideal gases", the activity (a) is defined below in equation (13):

$$a = \frac{P}{P^0} \quad (13)$$

where P = pressure or partial pressure of the gas and P^0 is the standard pressure. The activities of the reactants and the products modify the Gibbs free energy so that in a chemical reaction of the format in equation (14):



can be represented in the Gibbs free energy change of a reaction by equation (15) below:

$$\Delta g_i = \Delta g_i^0 - RT \left[\ln \left(\frac{a_j^j a_k^k}{a_L^l a_M^m} \right) \right] \quad (15)$$

The activity of the reactants increases as the change in the Gibbs free energy of formation becomes more negative (or more energy is released). This relationship can be substituted into the Nernst equation by using the relationship shown in equation (16):

$$\frac{-\Delta G^0}{RT} = \ln K(T) \quad (16)$$

where K, the temperature related equilibrium constant, can be defined as in equation (17):

$$K = \left(\frac{V_{products}^{v_{products}}}{V_{reactants}^{v_{reactants}}} \right) \left(\frac{P}{P_{ref}} \right)^{v_{products} - v_{reactants}} \quad (17)$$

The difficulty in using the Nernst equation for an accurate understanding of the resulting current is that the voltage will vary along the surface of the cell because of the concentration changes and the partial pressure changes. The effects then must be integrated along the cell. This is far beyond the defined scope of this project. Instead the Haynes curve from the reference “Simulation of Tubular SOFC behavior for integration into gas turbine cycles” was used to interpolate the cell performance at 1 atm.

In this case as discussed in the background, the difficulty of the integration along the length of the Fuel cell was assuaged by the use of C. L. Haynes’s model for TSOFC performance for pressures between 3 atmosphere and 10 atmospheres for a Siemens-Westinghouse fuel cell. The SOFC system used in this design will be operated at atmospheric pressure, so Haynes’s model had to be extrapolated down to one atmosphere.

Haynes's model establishes curves for cell operating pressures of three, five, and ten atmospheres. The need for this particular design is to operate at slightly greater than one atmosphere. An extrapolation is taken from Haynes's model down to one atmosphere by reading the measurements of amperage at two different voltages. To document the process, two voltages were chosen at 0.65 volts and 0.75 volts.

The results from these choices are shown in Table 2.

Table 2: Current from Hayness' pressure/ voltage chart

Voltage	.60 V	.75V
Pressure (ATM)	Current (Amps)	
3	335	190
5	360	215
10	395	250

Figure 9 shows a graphical interpretation of the data from the table and the extrapolation down to one atmosphere.

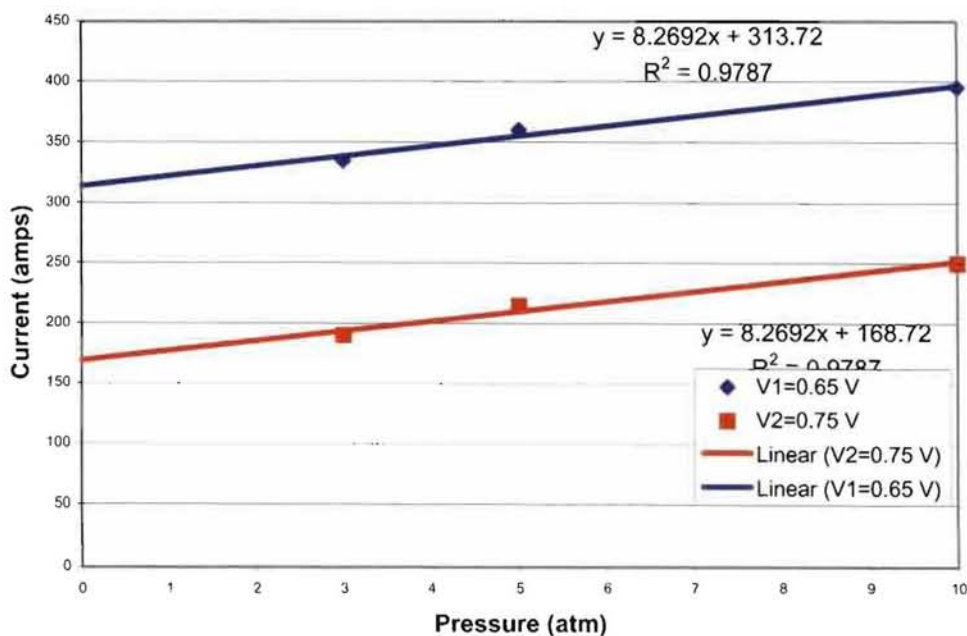


Figure 10: Cell current vs. operating pressure

Measurements are taken from the graph above at one atmosphere. These measurements are plotted and linearized in the following graph, figure 10.

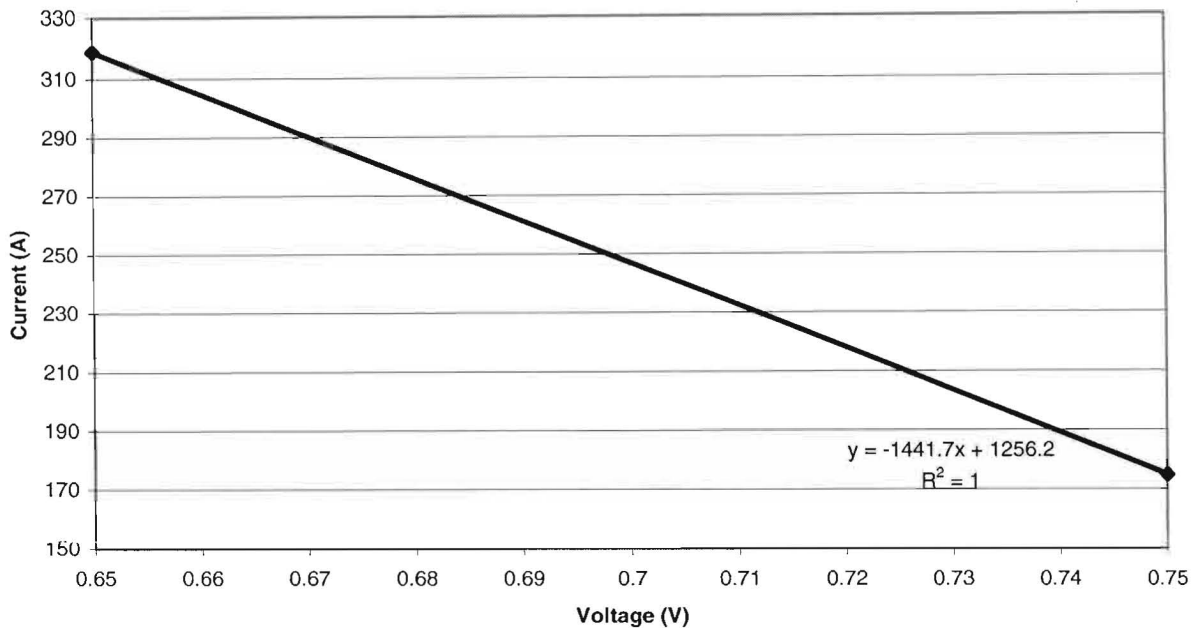


Figure 11: Predicted cell current vs. Cell voltage for TSOFC

The curve accounts for the changing Nernst voltage across the surface of the cell. It will be from this generalized curve that the cell performance will be estimated by establishing the equation that represents the relationship between current and voltage and provides the basis for the modeling of the overall power output of the fuel cell. With a value for the cell current, the overall cell power could be determined. Equation (18) is used to determine cell power.

$$P = VI \quad (18)$$

The power from one fuel cell is used to determine the number of fuel cells needed for the entire system by dividing the entire power required from the stack by the power of one cell as shown in equation 19:

$$\# \text{ of cells} = \frac{P_{\text{system}}}{P_{\text{cell}}} \quad (19)$$

The number of cells becomes extremely important in overall design because many key design factors are contingent upon this figure. In this design, the number of cells must be a factor of 11520 since that is the number of cells in a stack to be purchased from Siemens Westinghouse.

The molar flow rate of the fuel and the oxidizing stream needs to be determined as well, and this is done on a single cell basis as well. Fresh fuel is injected through an ejector nozzle that mixes with depleted gas from the upper zone of the fuel cell substack. This fuel mixture is directed to a pre-forming section where partial reformation occurs within a catalytic bed. The preponderance of fuel reformation occurs in the top of the stack and a hydrogen rich stream is fed at the base of the stack at the base to the exterior of the tubular cells. Complete reformation is finally achieved at the closed end of the fuel cell.⁵ The fuel in this design is methane. Using the current from the cell the mass flow rate can be determined by multiplying the power times the molecular weight of the fuel cell per amp. When multiplied by the total number of cells, the total flow rate can be determined.

In a fuel cell, there is a utilization factor that is used to account for the fact that all of the fuel is not consumed within the cell. This factor can be defined by equation 20 below

$$U_f = \frac{\text{fuel consumed}}{\text{fuel supplied}} \quad (20)$$

The total flow rate for the system is then determined from the Fuel Consumed divided by the utilization factor. To determine the air supply that was required by the system a similar process is used, basing the amounts of each of the

⁵ Lundberg p 48

components of the stream on the stoichiometric balance in the overall chemical equation.

In this design the oxidizer stream is made up of carbon dioxide, steam, oxygen, and nitrogen coming from the gas turbine. The molar flow rates of each of these components were needed at both the inlet and exit. They were found in a similar manner to that of the fuel.

Combustion Preheater

When combining the TSOFC with the gas turbine, there are some additional system characteristics that must be accounted for. The air coming into the fuel cell comes from the heated exhaust of the gas turbine. While the temperature is quite high, if this were to be taken directly to the fuel cell, the energy would be used in the cells to a point that it would not be possible to maintain the constant 1000°C. To make up for this, before the exhaust enters the fuel cell it is sent through a combustion preheater. In joining the fuel cell with the gas turbine and the heat exchanger, the energy balance must be understood across the fuel cell and preheater so that entering and exiting temperatures could be determined.

Examining first the fuel cell, the thermal sources included the energy transfers due to irreversibilities, and due to the hydrogen combustion. The sinks where energy is absorbed in the system are from the methane reforming, the energy transfer to the surroundings, and the energy transfer in the oxidizer stream heating. The diagram below depicts these transfers in the cell.

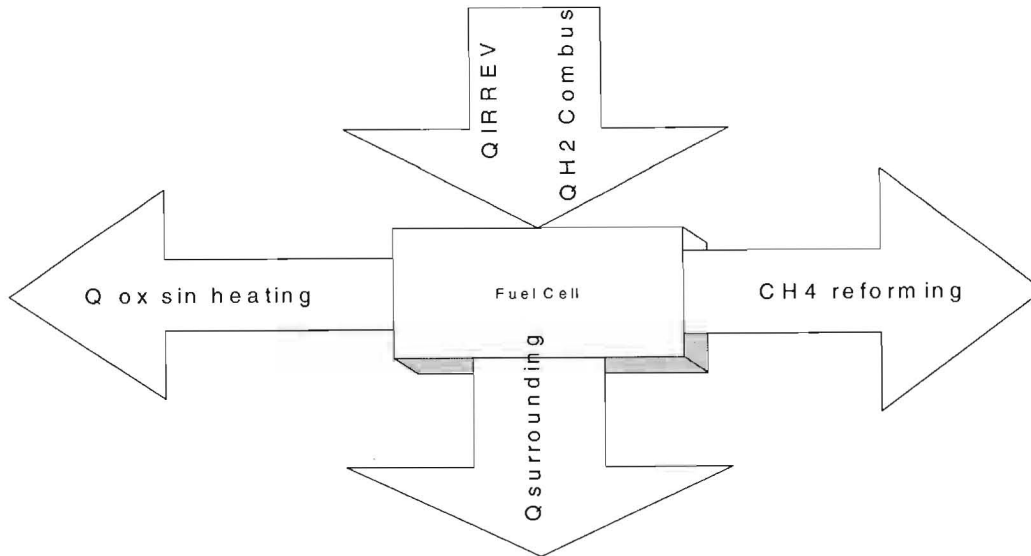


Figure 12: Fuel cell thermal sources and sinks

Looking at each of those as separate terms, the energy transfer representing the irreversibilities is equal to the following equation:

$$Q_{\text{irrev}} = P_{\text{cell ideal(rever)}} - P_{\text{cell, actual}} \quad (21)$$

Where the actual power was obtained from the current taken from the performance curves and the voltage was specified using $P=IV$. To find the reversible or ideal power, the lower heating value (LHV) of methane was used. The lower heating value is found where all the water formed by combustion is vapor.⁶ When taking the LHV and multiplying that by the molar flow rate of the hydrogen in the cell, the result can be multiplied by the current to find the ideal value for power.

For the oxidizing stream, the molar flowrates of the components of the oxidizer stream is multiplied by the change in enthalpies of the components of the oxidizer stream. As discussed previously, the oxidizing stream consists of carbon dioxide, steam, oxygen, and nitrogen. Since the oxidizer stream is coming from the gas turbine exhaust, the temperatures used to determine the enthalpies will be that with which the exhaust leaves the turbine and the 1000 degrees of the

⁶ Moran, p. 645

fuel cell. The resulting equation for the change in enthalpies is represented in equation (22):

$$\Delta h_{ox} = \Delta h_{CO_2} + 2\Delta h_{H_2O} + \left(\frac{\dot{n}_{O_2i}}{\dot{n}_{fb}} - 2 \right) \Delta h_{O_2} + 3.76 \left(\frac{\dot{n}_{O_2i}}{\dot{n}_{fb}} \right) \Delta h_{O_2} \quad (22)$$

where the molar flow rate of the oxidizing stream is equal to the molar flow rate of the expander as shown in equation (23).

$$\dot{n}_{ox} = \dot{n}_{expander} = \dot{n}_{f,b} \left(1 + 4.76 \frac{\dot{n}_{O_2i}}{\dot{n}_{f,b}} \right) \quad (23)$$

From information from Siemens Westinghouse, the energy transfer to the surroundings can be found by approximating two percent of the energy transfer due to irreversibilities. This has been shown to be true in research by Siemens Westinghouse as told to the design team in lecture.

The energy from the hydrogen combustion is found by multiplying the LHV of hydrogen by the change in the molar flow rate across the cell stack. The last of the energy transfers is found by making a control volume around the reformer using the first law for the reformer as shown in equation (24) below:

$$Q_{CH_4,ref} = \sum_{exit} \dot{m}_e h_e = \sum_{inlet} \dot{m}_i h_i \quad (24)$$

The energy transfers were important in determining the entering and exiting temperatures by balancing them, and were used as part of the fuel cell code to match up the other system components to the fuel cell.

Assumptions

Just as with the gas turbine there are many assumptions made to accurately yet with less difficulty model the fuel cell system. The steam reforming reaction and the water gas shift reaction are both assumed to go to completion. This gives a single overall reaction for methane and, based on that assumption, only hydrogen will undergo an electrochemical reaction in the cell. In reality, there would be some CO used. Other assumptions taken into consideration are the use of pure methane (CH_4) for fuel. Pure CH_4 is used for ease of calculation. In reality, CH_4 has a small amount of sulfur and that is added by the utility company for safety purposes. In the model, the fuel must go through a desulfurizer before it enters the fuel cell in order to eliminate the sulfur from the fuel. An unpressurized system is also assumed for the ease of calculation. A pressurized system most often produces a more efficient fuel cell, however the scope of this project did not include this. Many research papers are available to understand the effects of pressure.

Another important assumption allows for the elimination of a reforming chamber that would have increased cost. The assumption is that with the high temperatures the reforming reaction takes place within the fuel cell.

Using air as an oxidizer is more economical than using pure O_2 . No excess air in the fuel cell means that all reactions go to completion, of course since this system is married to a gas turbine the exhaust air from the turbine is the natural place to procure the air.

Modeling the TSOFC

The simplified model of the fuel cell begins with interpolation of the cells' performance curve. The entire model code can be found in Appendix A. The below diagram identifies the parts of the Fuel Cell in the overall system to facilitate the numbering sequence.

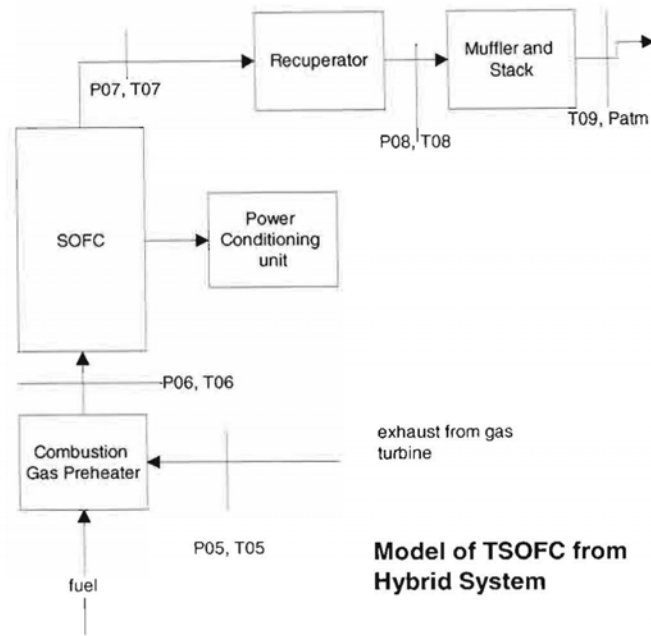


Figure 13: TSOFC process flow in hybrid system

To begin the interpolation, the pressure P08 is determined by assuming a value by using the following equation:

$$P08 = 1/(1-.01) \quad (25)$$

This represents the losses across the muffler and the stack, the pressure outside the stack is considered to be atmospheric pressure. Working backward from there the pressure losses across the recuperator is found in equation (26).

$$P07 = P08/(1-.01) \quad (26)$$

The pressure change across the heat exchanger is considered to be minimal as well and is found in a similar manner. Equation (27) represents how this pressure change is modeled in the hybrid system.

$$P06 = P07/(1-.01) \quad (27)$$

To use the Haynes's performance curves, the pressure at a single cell must be determined and this is done in the model using equation (28).

$$\text{CELLPRESS} = (\text{P06} + \text{P07})/2 \quad (28)$$

With this pressure, in the model a curve fit was determined using the Haynes data at two voltages $V1 = .6$ Volts and $V2 = .75$ Volts. The resulting current could be determined as shown in equations 29 and 30.

$$\text{EYE1} = 390 + 7.857 \times \text{CELLPRESS} \quad (29)$$

$$\text{EYE2} = 180 + 7.143 \times \text{CELLPRESS} \quad (30)$$

Where EYE1 and EYE2 are the cell currents in amps. The points can be "plotted" and the resulting curve fit equation allows for the cell current to be determined. Equation (31) is how this is represented in the code.

$$\text{EYECCELL} = \text{EYE1} + ((\text{EYE2}-\text{EYE1}))/0.15 \times (\text{VCELL} - .6) \quad (31)$$

Once the amperage resulting from a single cell was known, the power resulting from one cell could be modeled. This was done using equation (32).

$$\text{PCELL} = \text{EYECCELL} * \text{VCELL} \quad (32)$$

The amount of power that was necessary from the fuel cell had been determined and set constant. In this case the power was determined to 2.75 MW and was represented in the code by the term TOTPOWFC. To determine how many cells were going to be necessary to produce the total power prescribed the total power from the fuel cells was divided by the power from one cell. This figure would then be manipulated by making adjustments to the model to insure that the number of cells would be in a quantity that was available to be purchased.

After determining the power and number of cells, the modeling to determine the molar flowrates of the oxidizer and fuel streams and the actual exit temperature of the fuel cell had to be determined to effectively marry the fuel cell to the rest of the gas turbine components. This process began by determining the molar flowrate of the methane per cell. The model was set up in the same manner as was discussed in the previously documented section in which the molar flow rate was found for one cell and then was calculated for the entire fuel cell system. In the same systematic way the flowrate was determined for the oxidizer stream, then was broken down into each of the components of that stream, water, oxygen, carbon dioxide, and nitrogen. These flowrates were critical in the model of the recuperator.

The energy balance modeling to determine the temperature of the exhaust stream was also a critical factor in the modeling of the recuperator. To determine the true value at T06 an iterative loop had to be established. An initial guess was made that the value would equal the temperature of the gas turbine exhaust, T05. An energy balance was written into the code across the fuel cell and preheater to solve for the exhaust temperature.

Working backward toward the fuel

Analysis

Because of the use of the Haynes's Model, the modeling of the fuel cell was greatly simplified. The key outputs are identified in the following table

Table 3: Results from fuel cell code

Factor	Result
I_{cell}	398.057 AMPS
P_{cell}	23.88342 Watts
Total # of Cells	11520 cells
Molar flow rate of methane per cell	$0.6066922 \cdot 10^{-06}$ kmol/sec
Total Molar Flow rate of methane for the system	25.16192 kmol/hr
T06	784.56°C

The values obtained were realistic facsimiles of what could be expected from a Siemens Westinghouse fuel cell. This was important in the rendering the validity of the overall system. The system inputs including temperatures, the power ratio between the fuel cell and gas turbine, were manipulated to insure that the number of fuel cells in the stacks matched the product availability made by Siemens Westinghouse. The future steps of exploration using this model could include manipulation of the pressure of the system to increase the efficiency, but such is outside the scope of the present study.

Many of the results in this report have been produced by other sources. In that vein, this design does not provide new information on fuel cells but instead it was an exercise in validating the code.

Recuperator

Background

A heat exchanger is any of several devices that transfer heat from a hot to a cold fluid. In many engineering applications, it is desirable to increase the temperature of one fluid while cooling another. A number of methods are used to recover heat from exhaust flows such as ventilation air from buildings, damp, hot air from dryers, or waste gases from burners. All these methods are designed to exploit the temperature difference between exhaust and supply flows to the stream using as little material and fan energy as possible. The most common methods are recuperators such as crossflow and counterflow plate exchangers. In a recuperator, this takes place without interim storage of the heat and the two fluid streams do not mix. For this reason, a recuperator is preferable for a great many processes. Figure 14 depicts the method of heat transfer and flow in a recuperator.



Figure 14: Heat exchanger in a recuperator

Recuperators are categorized as parallel flow, crossflow and counterflow heat exchangers. In a parallel flow recuperator, the airflows are separated by the partition walls of the recuperator and move in the same direction. If the wall is extremely large and, provided the thermal capacity flows are equal, the output temperatures of both flows will be equal at half the input temperatures. The effectiveness of a recuperator is defined as the ratio between the temperature difference in one of the flows (the largest when the thermal capacity flows are not equal) and that of the input temperatures. The effectiveness of a parallel flow

recuperator can, therefore, never be more than 50 %. For this reason, it is desirable to utilize a type of recuperator that is more efficient.

The most common recuperators are crossflow plate heat exchangers [4]. Figure 15 shows a plate crossflow heat exchanger.

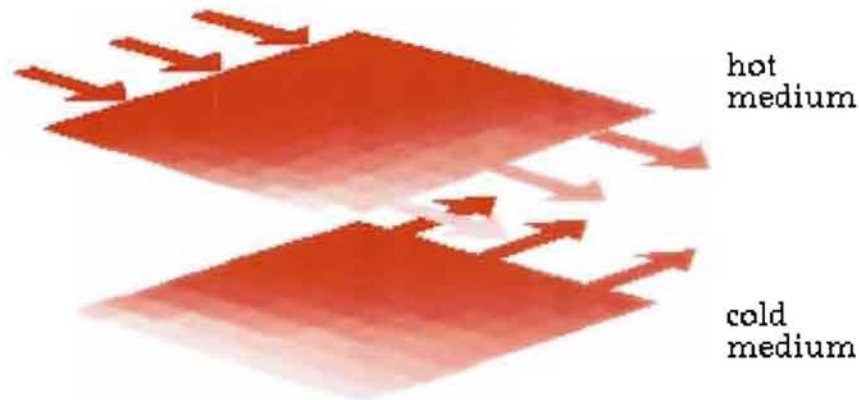


Figure 15: Crossflow recuperator

In crossflow heat exchangers the directions of the fluid velocities are generally at right angles to each other although numerous other configurations exist. Additionally, crossflow exchangers can be classified according to whether each stream remains mixed or unmixed as it passes through. The flows of most compact crossflow heat exchangers are exactly, or are very nearly, unmixed. Since this is the case, the unmixed configuration has received most attention.

Of major importance in any type of heat exchanger are the temperature gradients of the two streams. Achieving a desired rise or drop in temperature is the sole purpose for utilizing this type of equipment, after all. For simplicity's sake, the temperature distribution within a recuperator is usually assumed to be two-dimensional. That is, the temperature varies longitudinally in the heat exchanger streams, but it is constant throughout the cross-section of the flowing stream.

Figure 16 shows a general temperature distribution for a crossflow heat exchanger.

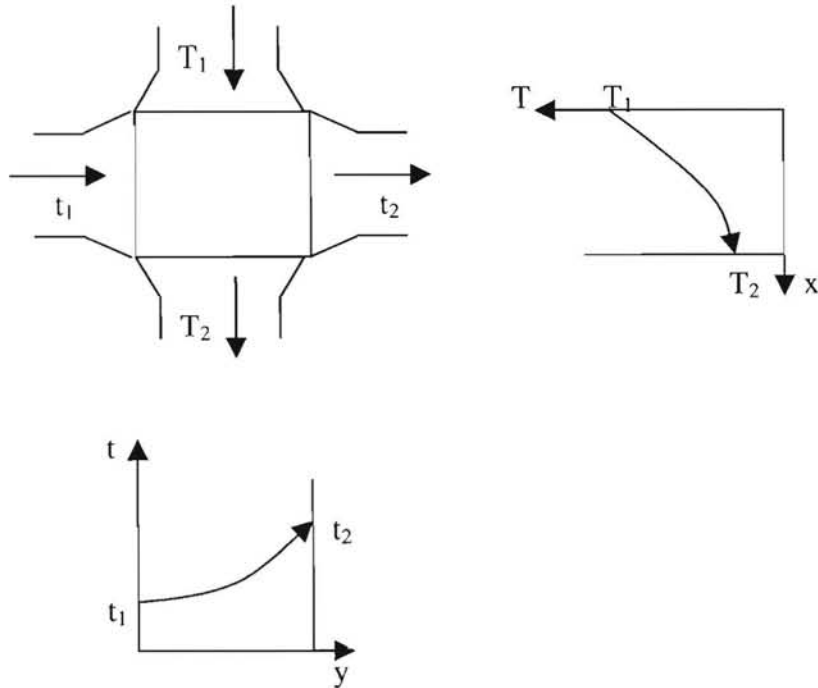


Figure 16: Temperature profiles for flow in a crossflow heat exchanger

Because of the two-dimensional nature of the temperature distribution, the actual temperature gradients as shown in Figure 16 are higher than those of a counterflow unit, but since crossflow exchangers are generally designed for much lower effectiveness and hence lower NTU's the loss of effectiveness is usually small.

Recuperator Model

For this design, an effective recuperator is of major import. The objective of this heat exchanger is to recoup the excess heat energy coming from the fuel cell exhaust. This heat exchanger will transfer the energy taken from this stream to the compressed air of the gas turbine to pre-heat it before it enters the combustion chamber. By recovering this thermal energy the overall efficiency of the cycle will increase due to the decrease in required fuel consumption in the gas turbine burner. Since heat transfer will take place between two gases, a

crossflow design was chosen because the crossflow design is the most effective for that type of flow situation [1]. For the initial calculations it was assumed that both streams were unmixed [2]. Crossflow exchangers are subject to fouling, as are other exchangers, but it is difficult to apply fouling-factor values to the area in a crossflow exchanger [3]. Consequently, the analysis will not consider fouling effects in crossflow heat exchangers. Other assumptions made for the design were air is an ideal gas, the cycle is operating at steady state, kinetic and potential energy effects are negligible, and specific heat of fuel cell exhaust can be approximated as super-heated water vapor. The overall heat transfer coefficient U is a constant over the length of the exchanger. It is assumed fluid properties are constant. Finally, it is assumed that there are no heat losses; that is, all heat transferred from the warmer fluid goes to the cooler fluid.

In order to determine the design parameters of the recuperator, a model of the heat exchange process in a crossflow type exchanger needed to be developed. There is available in *Compact Heat Exchangers* by Kays and London an excellent summary of test on crossflow heat exchangers. A number of conventional types have been tested for heat transfer and friction characteristics [1].

In this study, only the inlet temperatures of the two streams are known so the effectiveness—NTU method was used to calculate the results. This method relies on finding the heat capacity rate, C [2].

$$C = \dot{m} c_p$$

where,

\dot{m} - Mass flow rate of stream

c_p - Specific heat of fluid

The ratio of capacitance, R_c , is defined as

$$R_c = \frac{C_{\min}}{C_{\max}}$$

can then be found. Effectiveness, ε , was then found by the equation:

$$\varepsilon = 1 - \exp[R_c (NTU)^{0.22} \times \{\exp[R_c (NTU)^{0.78}]\}]$$

(crossflow, both fluids unmixed)

The number of transfer units NTU was chosen in a range of $1 \leq NTU \leq 2$.

Using the values of the expressions above, the outlet temperatures of the exiting hot stream T_{he} and exiting cold stream T_{ce} can be found as follows.

$$T_{he} = T_{hi} - \varepsilon R_c (T_{hi} - T_{ci})$$

and

$$T_{ce} = T_{ci} - \varepsilon C_{max}/C_{min} (T_{hi} - T_{ci})$$

where $T_{c,i}$ is the temperature of the entering cold air stream coming from the compressor and $T_{h,i}$ is the temperature of fuel cell exhaust stream.

A typical value of the overall heat transfer coefficient U was chosen. All the information needed to calculate the area of the heat exchanger A_{HEX} is now known. This calculation is carried out using the following equation.

$$A_{HEX} = \frac{(C_{min})(NTU)}{U}$$

In the modeling of the recuperator for the atmospheric pressure hybrid cycle power generation system the following input values were known or assumed:

Specific Heat of CO_2 in KJ/Kg-K: 0.846

Specific Heat of H_2O in KJ/Kg-K: 1.8723

Specific Heat of O_2 in KJ/Kg-K: 0.918

Specific Heat of N_2 in KJ/Kg-K: 1.039

Mass Flow Rate of Air in Kg/s: 5.69

NTU: 1.5

U in KJ/H-K-M²: 100

Inlet Temperature of Air to the HEX in Kelvin: 298

Total Mass Flow Rate of Exhaust in Kg/h: 169.36

Using the above information, the FORTRAN model was able to find the unknown quantities of importance. The outlet temperature of the exhaust gas stream was found to be 907.7 K while that of the compressed air stream going to the combustion chamber was 980.4 K. To achieve these temperature changes, a heat exchanger area of 544.1 m² was required.

Other Plant Equipment

Although they were not included in the modeling for the plant, many other key components exist in a power plant such as the one under consideration here. This discussion will not be an in-depth one, but it should give a good idea of what the systems are and why they are important to the plant.

Fuel Processing System

The natural gas that comes from the main gas pipeline must go through several processes before it is ready to enter the hybrid power system. First, the pressure of the fuel must be dropped to that which is required by the system. This can be done in many different ways, but for the purpose of this study, it is assumed that the fuel passes through a diffuser where the pressure reaches the desired level. Next, the fuel must be filtered to remove any contaminants that might poison the fuel cell or gas turbine. The contaminant of most concern at present is sulfur. This material, in the form of mercaptan, is added to natural gas at local utility distribution stations to add odor for safety purposes. Since sulfur is very detrimental to both the fuel cell and the gas turbine expander, not to mention the environment, it will be removed using a desulfurizer. After desulfurization, the fuel is ready to enter the two combustion chambers and the fuel cell. As part of the fuel processing system, and the desulfurization process in particular, a hydrogen supply system is necessary to active the catalyst in the desulfurizer.

Nitrogen Supply Systems

This system is one that has been implemented for safety reasons. Nitrogen is stored in pressurized cylinders until it is needed. In the case of an emergency where it is necessary to shutdown the plant very rapidly, nitrogen would be forced into various areas of the plant to purge the system of natural gas, thereby stopping all reactions, combustion and chemical.

Startup Boiler

This system is necessary to start the plant back after a shutdown. It consists of a boiler, powered by combusting natural gas, that sends steam to the turbine to start the turning of the expander, thus supply shaft power to the compressor and beginning the entire system of power production. It is impossible to start the plant without this type of system.

Auxiliary Air Compressor

This component stores compressed air in an accumulator and serves as a protective measure for the TSOFC. In the event of a plant shutdown, the auxiliary air system will cool the fuel cell generator system down from the operating temperature to one that is less detrimental to the integrity of the system.

Power Conditioning Unit

For the power system performance estimates, the power conditioning efficiency, pertaining to the process between the SOFC DC terminals and the utility AC grid, was assumed to be 94%. This is consistent with current Siemens Westinghouse study of power generation products to be offered around 2010. Siemens Westinghouse recommends locating the PCS immediately outside of the SOFC.

By converting the DC power to AC at the SOFC, the length of the high current DC bus duct, and the number of high current DC electrical components can be minimized. According to Siemens Westinghouse's report medium voltage components are more readily available, smaller, and less costly than low voltage, high current DC components.

Based on the findings of Siemens Westinghouse, the PCS should be configured to supply continuously adjustable current. The output power factor will also be adjustable from leading to lagging power factor. The PCS should be designed to tolerate some level of phase imbalance. The PCS will manage the export power based on the set points transmitted from the SOFC control. Included in the system are a DC to AC inverter and a setup transformer. The DC to AC inverter converts the high current DC power into 480V, three phase AC for distribution. The transformer boosts the voltage for greater distribution efficiency and reduced bus conductor requirements.

The Siemens Westinghouse SOFC/GT electrical distribution system links the SOFC module and the gas turbine system to the power conditioning system (PCS), and the power conditioning system to the utility AC power grid. Included in this setup are the bus leads, all of the power monitoring equipment, disconnect switches, and protective devices. A setup transformer is supplied as part of the PCS to elevate the output voltage before it is routed to the switchyard. At this switchyard additional step-up transformers raise the voltage as necessary for export to the utility grid. The disconnect switches will be strategically located for safe operation and maintenance of the SOFC. Fault detection equipment will be provided, to sense utility grid under voltage, over voltage, and off frequency conditions.

The electrical power from the SOFC modules can be exported to the utility grid via a 13.8 kV bus if the adjacent grid lines are at this voltage. Otherwise, setup transformers in the switchyard are used to match the voltages. A static isolator will be provided between the high voltage bus and the grid interconnection to allow for quick disconnect, in the event of a fault, either on the utility grid, or on

the SOFC generating system. In Siemens Westinghouse individual SOFC, sub modules are protected by three phase circuit breakers.

The performance of the electrical distribution system is closely monitored by and controlled the instrumentation and control system. The instrumentation and control system provides the supervisory functions for power flow and fault conditions for each SOFC sub-system and the gas turbine systems.

While the above plant systems and components are not taken into consideration during system modeling, they are nonetheless integral parts of this operation. Without them, the hybrid power system could not run safely and effectively. Thus, their mention here is merited.

Economic Study

Before the final decision of whether or not to proceed with a project of this type can be made, an economic analysis must be performed to determine its feasibility. For this particular project, it was decided that this analysis could best be done by using the present worth (PW) method, which takes a series of cash flows over the life of a project and discounts them back to the present to determine if the project is economically sound. A project with a negative PW is not a good investment while one with a positive PW is sound. The equation used to determine the PW for the project is as follows

$$PW(i\%) = \sum_{k=0}^N F_k(1+i)^{-k},$$

where “k” indicates the period in question and “N” is the total number of periods in question. For this project, “N” will be equal to thirty, since the projected life of the plant is 30 years. Furthermore, “F_k” represents the amount of the cash flow for each period, k. Finally, in the preceding equation, “i” represents the effective interest rate for the project.

The interest rate that will be used in this study is equal to the MARR (16%) for the project. The MARR is the absolute minimum return that a company will accept on its investment. Thus, a MARR of sixteen percent means that the company expects to earn (or save) sixteen percent of what they invest in a project, or they will not participate. Each company determines their MARR in a different way, so it is extremely difficult to find some set way of finding this number. Thus, an estimation of a good value for the MARR had to be made using available data. In doing so, several factors were taken into consideration. First, the average return on investment for the S&P 500 over the past fifty years was examined to see how much the customer could reasonably expect to make by simply investing its resources in the market. This research yielded a rate of thirteen percent. Next, the minimum acceptable return for individual investors was found. This number was determined to be between ten and eleven percent. Finally, the MARR must be greater than the interest rate the customer will have to pay on the capital that is borrowed to complete the project. This number will vary depending upon the customer's credit rating and the type of project in question, along with several other factors. After

taking all of this information into consideration, it was determined that the best course of action was to set the MARR at sixteen percent. This interest rate will allow the customer to have a greater return on investment than if it merely invested in the market, but it also sets expectations at a reasonable level so that the project will not automatically be discredited as unprofitable.

Once the MARR was determined, the amount of the cash flow at the end of each year of the plant's life had to be found. This included everything from the capital costs at the beginning of the project to the salvage cost at the end of the plant's life. While these two values are paid once during the plant's life, there are many other costs, such as maintenance and fuel, which occur every year. To ensure that all cash flows were taken into consideration, a list of costs was drawn up using the paper written by Siemens-Westinghouse after their similar study as well as books that deal with engineering economy and cost estimation.

The major sources of cash flow are capital costs (equipment, piping, buildings, etc.), yearly operating and maintenance costs (salaries for operators and maintenance personnel, unexpected repairs, etc.), fuel cell replacement costs (occur every six years), and fuel. The only source of revenue (savings) for this project is the money saved by not purchasing electricity from a local utility. Many of the yearly costs, such as taxes and depreciation are a function of the total capital investment in the project, so the data necessary to estimate the necessary capital of the project cost was found first.

The basis for all capital costing was the aforementioned Siemens-Westinghouse paper. In its study, Siemens modeled a 19 MW plant, which is obviously much larger than the plant under consideration in this study. Thus, a scaling operation had to be undertaken to reduce the costs Siemens published to those that corresponds to a 4.3795 MW operation. The capital cost estimates for the 19 MW plant, which are all based upon mature technology, are shown in Table B1 in the appendix.

To make the data in Table 4 fit the smaller plant, several things had to be done. First, the SOFC generator system and SOFC power conditioning system costs were divided

by 16.571, which is the total fuel cell power output in the Siemens system. This number was then multiplied by 2.7515 to determine the cost of the fuel cell system in this design. All of the numbers for the fuel cell system were scaled back using this method, but, in reality, the cost of freight and installation would probably not be determined in this way; rather, the vendor would give a quote for these things that depended upon the distance the equipment had to be hauled and the amount of time required to install it. For the sake of this cost analysis, however, it is assumed that they can be calculated in this manner. Further, the turbine cost data was scaled down in the same manner as the fuel cell costs. The difference came in the numbers used; the Siemens study used a 4 MW gas turbine while this project calls for a 1.628 MW unit. These two numbers were used to find the estimated cost for the gas turbine used in designing this system. Most of the other cost data in the Siemens study was scaled back using the total power outputs of the two systems (19 MW and 4.3795 MW).

It should be noted that the cost of land and a switchyard was omitted from the present study due to the lack of need for them. It is assumed that the customer already owns the very small portion of land that will be required for this plant. Moreover, since this power system will not be connected to an electrical grid, there is no need to have a switchyard into which to dump the electricity that is produced. Another difference between the two studies comes in the lower portions of the two tables. Rather than scaling down the cost of site preparation and R&D, G&A, etc., costs, a number was assumed for these quantities. This was done for several reasons. That particular cost number included research and development costs. For the purpose of this study, it is assumed that all R&D costs were paid by corporations, such as Siemens-Westinghouse, that are in the business of designing new power systems. Also, there is no real need to include the costs of sales and marketing for this project since nothing will be sold; rather, the power produced will be used in-house. Finally, the profit allowance should not be included in this section. That part of the project will be taken into consideration later in this study. Thus, only \$200,000 is assumed for this category in the cost estimate Table 5 lists the capital costs, as calculated in the manner detailed above, for the hybrid system requested by the customer.

Table 4: Capital cost estimates for a 4.3795 ME hybrid system

Installed Equipment Costs					
	Equipment	Freight	Installation	Totals	
SOFC Generator	1,476,193	5,230	7,865	1,489,288	
Gas Turbine System	1,611,998	1,425	24,154	1,637,576	
SOFC Power Conditioning System	330,180	2,615	4,047	336,842	
Instrumentation, Controls, and Electrical Cabinets	202,273	1,614	45,989	249,876	
Switchyard and Electrical Distribution	0	0	0	0	
Fuel Supply System	38,514	403	2,305	41,223	
Hydrogen Supply System	20,694	403	2,305	23,402	
Purge Gas Supply System	27,780	403	2,305	30,488	
Auxiliary Air Supply System	41,426	403	1,501	43,330	
Startup Boiler System	17,261	403	303	17,967	
Piping and Insulation	370,656	3,630	73,218	447,505	
Site Buildings				8,335	
Totals	4,136,976	16,531	163,992	4,325,834	
Project Cost Summary					
Installed Equipment					4,325,834
Project Management, Engineering, and Permitting					199,257
Site Preparation					57,922
Grading, utilities installation				0	
Foundations installation				47,144	
Structural steel installation				10,778	
G&A, R&D, Sales & Marketing, Profit Allowance					200,000
Total Plant Cost					4,783,013
Spare Parts Allowance					53,514
Startup					32,510
Land					0
Total Capital Requirement					4,869,037

As can be seen in a comparison of the bottom line of the two tables, the capital requirement of the 4.3795 MW is approximately one-fourth of that of the 19 MW plant.

Once all the capital costs have been tallied, the price tag on physical assets for this plant is \$4,869,037. This corresponds to a capital cost of electricity of \$0.13/kWh.

The next step in the cost analysis process was the estimation of yearly costs associated with operation and maintenance. These costs include fuel and catalyst costs, salaries for operators and maintenance personnel, gas turbine maintenance, and fuel cell replacement costs. The manner in which each was calculated will be described below.

First, the cost of operation and control of the plant was calculated. It was assumed that one operator would be required round-the-clock for fifty weeks per year. (A two-week shutdown period for maintenance is assumed.) The hourly wage for the operators will be \$38 per hour, which leads to an annual income of \$76,000. This number is actually above average for an engineer in the Knoxville area, so it seems quite reasonable. A further assumption that affects the cost of operation is housekeeping maintenance on the system. This would include small jobs that are required for the upkeep of the plant. An estimate of 20 hours per week was made for these duties. Maintenance and janitorial personnel earning \$15 per hour will carry out such tasks. Finally, administrative costs amounting to thirty percent of the total operating and housekeeping costs were assumed. All of these yearly costs were then divided by the total electrical output, in kWe, of the plant to determine the cost of electricity (COE) for operation in \$/kWe for a single year.

The next set of costs that was assessed was that for gas turbine maintenance. These costs were easily estimated using information gained from the Siemens report which estimates that the gas turbine maintenance cost as 0.01\$/GT-kWh. This number was multiplied by the turbine power output in kWh to determine a yearly cost, which was divided by the total output of the plant in kWe to find the final cost of electricity of turbine maintenance.

Next, the cost of adsorbents and catalysts for the fuel desulfurizer had to be found. Siemens estimated that the yearly cost for this would be approximately \$9,000 per year. Since the system they designed was so much larger than the one examined in this study, it would require a much greater fuel flowrate, and thus a greater capacity to

remove the sulfur from the fuel. For this reason, the cost of catalysts and adsorbents for this design (approximately \$2,000) was estimated to be much lower than in the Siemens study. Again, this number was divided by the total capacity of the plant to determine the COE in \$/kWe.

Another significant cost that is associated with a plant of this type is fuel cell replacement costs. Fuel cells have a very short life in comparison to gas turbines and other equipment in this system. Optimistic estimates list the replacement interval for fuel cells as every ten years, but a more realistic time frame is six years. Thus, in a thirty year plant life, the fuel cells will have to be replaced four times. The cost for the replacement of each fuel cell module, according to Siemens-Westinghouse, is \$468,920. This number will include the actual cost of the cells as well as the labor and time necessary to implement the change. In this plant, there will be only one module of cells. Although this cost will only occur every sixth year, its impact upon every year of the plant's life was found in this study. To do so, the above replacement cost of the cells was multiplied by 1.06 (assuming a six percent interest rate on the money borrowed for the replacement costs), and then divided by the total power output of the plant. This calculation yielded a replacement cost for each replacement period. This number could then be divided by the replacement interval to obtain a yearly COE of replacing the fuel cells.

By a large margin, the major cost for this project will be that of the fuel required to run the gas turbine, SOFC generator, and combustion gas heater. This cost was found using mass flowrates of fuel generated by the Fortran code along with heat rate calculations. This method of calculating fuel costs, which was found in the Fuel Cell Handbook, calls for the mass flowrate of methane, in lb_m/h , to be multiplied by a conversion factor of 21,597 Btu/ lb_m and then divided by the total power output of the plant, in kW. Multiplying the result of this calculation by the cost of methane in \$/MMBtu and dividing it by a factor of 1,000 yields the cost of electricity for fuel in \$/MWh. This COE could then be converted to the form of \$/kWe. The cost of methane that was assumed for this project was \$3.5/MMBtu. It was reached by examining the price of methane energy futures in the market today as well as by looking at the price Siemens assumed in their mature technology calculations.

Table 5: Yearly COE associated with plant operation and upkeep

COE Calculation Basis			
No. round-the-clock power system operators	1	SOFC replacement interval, years	6
No. plants on system	3	Desulfurizer adsorbent & catalyst, \$/year	2,000
Operator labor cost, \$/man-hour	38	Interest rate (SOFC replacement cost calculation), %	6
Housekeeping maintenance, man-hours/week/system	20	Power system efficiency (net AC/LHV), %	52
Housekeeping labor cost, \$/man-hour	15	Gas turbine methane mass flowrate (lbm/hr)	355.2511
Hours of operation each year	8400	Preheater methane mass flowrate (lbm/hr)	91.49393
System rating, MW net ac	4.3795	Fuel cell methane mass flowrate (lbm/hr)	889.9315
Gas turbine rating, MW net ac	1.628	Total mass flowrate of system (lbm/hr)	1336.677
SOFC module rating, MW dc	2.7515	Total heat rate for plant (Btu/kWh)	6591.666
Gas turbine maintenance cost, \$/GT-kWh	0.01	Fuel Cost, \$/MMBtu	3.5
SOFC replacement cost, \$/SOFC generator module	468,920	Total fuel cost (\$/MWh)	23.07
Cost Summary			
Fixed O&M, \$/kWe		Variable O&M, \$/kWe	
Plant operation & control	24.30	SOFC replacement	18.92
Housekeeping maintenance	3.56	Gas turbine maintenance	31.23
Administration (30% of operation & maintenance labor)	8.36	Desulfurizer adsorbent/catalyst replacement	0.46
Total Fixed O&M, \$/kWe	36.21	Fuel COE	193.79
		Total Variable O&M, \$/kWe	244.39
		Total COE, \$/kWe	280.61

The bottom line in Table 5 shows the cost of electricity due to variable costs to be equal to \$280.61 per kWe for each year of operation. This corresponds to a total variable cost of electricity of \$0.033/kWh, which will be multiplied by the total yearly power output of the plant to find the total variable cost for each year.

With the capital and variable costs already determined, the next step in the economic analysis is to determine the revenues for the project. Since the customer will not be selling the power it produces, these revenues take the form of savings due to producing power rather than buying. The cost of buying power is found by multiplying the plant's

capacity by the number of hours it operates each year and by the cost of electricity, in \$ per kWh. Since the plant is located in Knoxville, TN, which is in the distribution area of the Tennessee Valley Authority (TVA), the cost of buying electricity is very low. Knoxville Utility Board (KUB) lists the price of buying the power needed as \$0.0665/kWh. This translates to a total savings of \$2,446,388.70 per year. This number must overcome the total cost of electricity in each year with enough left over to pay off the capital costs if the plant is to be profitable.

To find the yearly cash flows for this project, several steps were taken. First, the gross cash flow was found by subtracting the total yearly cost from the total savings. Next, depreciation on the capital equipment was taken into consideration. A straight-line depreciation of 5% was assumed. This percentage was determined by taking the total capital investment for the project less the salvage value and dividing it by the depreciable life of twenty years. The plant is assumed to have zero salvage value at the end of its life. What the scrap from the machinery is worth will be used up in transporting it off the premises. This number could then be taken as a percentage of the total value. Upon this calculation, the rate was found to be the aforementioned 5%. Depreciation expense was factored in by multiplying the total capital cost by the depreciation rate. Since the depreciation was assumed to take place in the first twenty years of the plant's life, the last ten years will have zero depreciation expense. Subtracting the amount of depreciation expense from the gross income yields the income before taxes are applied. A tax rate of 30% was assumed for the customer; this number includes all local taxes as well as state and federal corporate income taxes. While the actual tax burden may vary somewhat from this rate, thirty percent is a reasonable estimation of the amount of tax that a corporation will have to pay. After the taxes were subtracted from the income before taxes, the depreciation expense was added back into the total yearly income. This was done because the depreciation must be figured into tax calculations, but does not actually lower the net income. Once this addition was made, the net income of each year of the plant was found.

It was the net income that was used as the cash flow for each year. These values were entered into the present worth equation mentioned above to be discounted back to the present in order to determine whether or not the plant was economically feasible.

According to this model, the project described in this study will save the customer \$2,289,073.47 over the course of the plant life. The total cost of electricity for this system is \$0.163/kWh. Appendix B contains a copy of the Excel spreadsheet that was used to perform the present worth study for the project.

It should be noted that the assumption of mature technology and prices was vital to the economic success of this project. Had present conditions been used in the study, the project would have lost a huge quantity of money. A great deal of this discrepancy can be explained by the fact that mature fuel cell technology costs are approximately one sixteenth of what they are now. Thus, purchasing and replacing the TSOFC generator system alone would have made the plant unprofitable had current prices been used. A majority of the explanation for the fact that the plant would have failed from an economic standpoint using current prices is its location. The price of purchasing electricity in the distribution area of TVA is so low that it takes an extremely efficient and low-cost power production system to be more cost effective than purchasing power from a utility. In fact, if the customer were to purchase power directly from TVA rather than going through a local utility (KUB), the plant would probably be unprofitable, even with the use of mature technology.

Environmental Impacts

The location of the design plant is in Knoxville, Tennessee, which is on the list of the top ten most polluted cities in the United States. The General Accounting Office reported last May that air pollution in the Southern Appalachian region originates from Midwestern industries as well as from the Tennessee Valley Authority's 11 coal-fired power plants in Tennessee, Alabama, and Kentucky. Knoxville's topography also contributes to its poor air quality. The series of valleys and ridges within the Knoxville landscape traps pollutants and does not allow these pollutants to be diluted. Figure 16 shows the air quality index of Knoxville, Tennessee for the past two years. These measurements were taken by Knox County Department of Air Quality Management between the months of May and September of the year 2000 and 2001, which are typically the peak months for air pollutants.

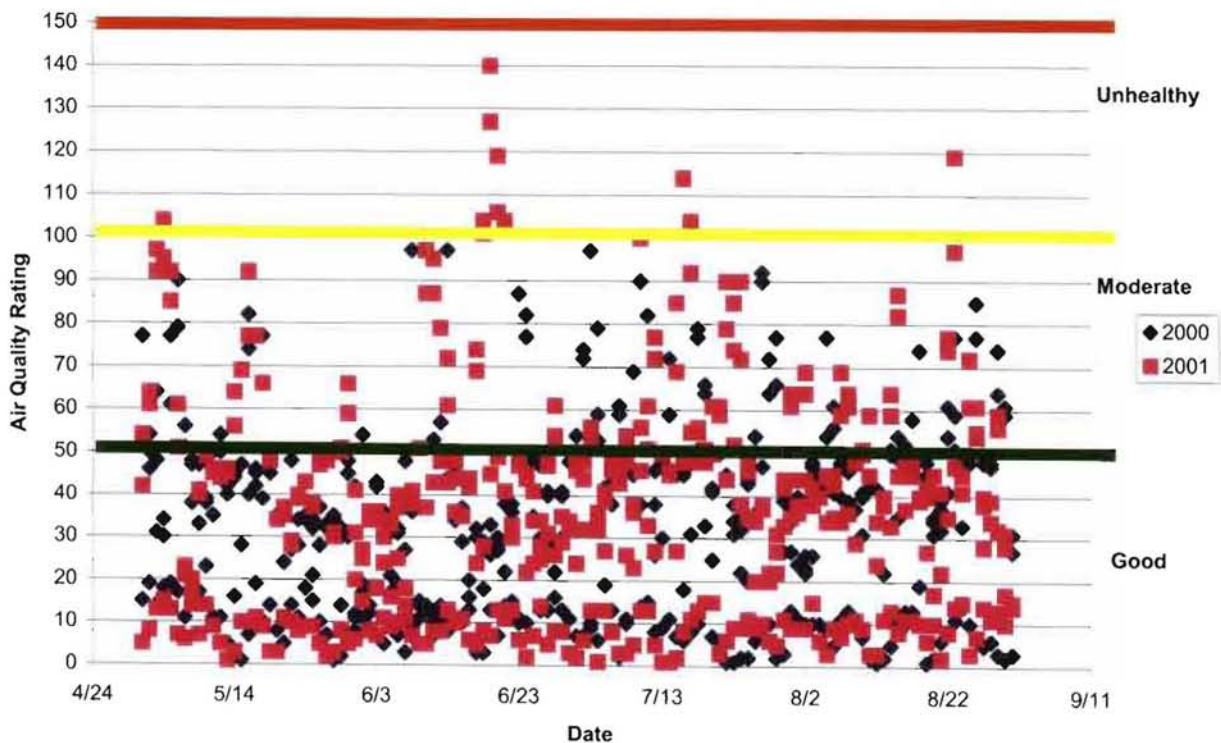


Figure 17: Air quality index of Knoxville between May and September

As shown by the graph, Knoxville's air quality is getting worse each year. Most of the moderate and unhealthy marks are from 2001. With heavy industries moving into the area and a constantly growing population that depends on internal combustion powered vehicles, the air quality in Knoxville is only going to get worse. To protect the citizens and environment in the area, something must be done to improve, or at the very least maintain, the air quality in the Knoxville area.

One very significant way in which this can be accomplished is to change the methods whereby power is produced to those that are more efficient in the use of fossil fuels. The benefits of this change will be two-fold. First, a more efficient system that burns less fossil fuel will produce fewer greenhouse gas emissions, thereby improving the quality of air. Second, the use of less fossil fuel will help to prolong the supply of these precious resources. This is especially important when the current political atmosphere in the Middle East, the origin of much of the world's supply of fossil fuels, is taken into consideration. The type of system that has been examined in this study is a major step toward the power production methods that are required to achieve this goal. While this type of system will still emit some greenhouse gases, the volume of pollutants will be a great deal less than is emitted by the type of power plants already in operation. Other than this relatively small amount of greenhouse gas, the only pollution that the plant will dump into the atmosphere is of the thermal type. Thus, the use of a hybrid fuel cell/gas turbine power plant will definitely help to reduce unwanted air pollutants, thereby improving the health of the environment in the Knoxville area.

Conclusion and Recommendations

The future is promising for the field of Gas Turbine and Solid Oxide Fuel Cell Hybrid power plants. This simple modeling, while rudimentary in form, was an outlet for more in-depth insight into the basic design steps that must be considered when considering power generation in the years to come. However if this plant would have to be built today, the investment, to be profitable would have to be judged against intangibles such as the value in research potential.

This model provides a basis for this design team to understand the thermodynamic relationships between systems in a hybrid power plant. While assumptions made calculations easier, to truly manipulate the codes that were written required a greater in depth understanding of the fundamentals of fuel cell and gas turbine design.

While no new ground was charted in the area of fuel cell research in this design, the outputs of the gas turbine and fuel cell were consistent with other similar research efforts. The overall system efficiency of 52% that was found agreed with earlier research efforts in this field. This efficiency carried with it a flowrate of 37.79 kmol/h of pure methane gas. Had the methane actually available for purchase been considered instead of assuming pure CH₄, the system efficiency would not have been as high and the flowrate of fuel would have be quite a bit higher.

It is the recommendation of this team that given mature technology the marriage of the European Gas Turbine and a complete stack of 11250 fuel cells could provide an output capacity well within the 3-5 MW range that was required. In the short term however, the price of gas in Tennessee and the available alternate sources of power make this entire system less feasible. Should the contract inspiring this design project be accompanied by a sizeable Department of Energy grant, it may be more feasible to advance into this technology at this time. There is much to be learned from the research of these types of system, this design was a good introduction to those fields.

Bibliography

1. Cirkel, Dr Hans-Jurgen. Siemens AG, Power Generation. "SOFC Fuel Cells and Gas Turbines: A Marriage of Efficiency" Freyestebenstr. Erlangen, Germany. 2001.
2. EG&G Services, Parsons Inc. Service Applications International Corporation. "Fuel Cell Handbook." Contract No. DE-AM26-99-FT40575. United States Department of Energy. Morgantown, West Virginia. October 2000.
3. Hesselgreaves, J. E. "Compact Heat Exchangers: Selection, Design, and Operation" 1st ed. Elsevier Science Ltd, Oxford, 2001
4. Incropera , Frank P. and DeWitt, David P. "Fundamentals of Heat and Mass Transfer." 4th ed. John Wiley & Sons, Inc., New York, 1996.
5. Janna, William S. *Engineering Heat Transfer* 2nd ed. CRC Press LLC, Boca Raton, 2000.
6. Korakianitus & Wilson. "Models for Predicting the Performance of Brayton-Cycle Engines", ASME Journal of Engineering for Gas Turbines and Power, Vol. 116, (1994).
7. Lundberg, W. L. G. A. Israelson, R.R. Moritz, S. E. Veyo, R.A. Holmes, P.R. Zafred, J. E. King, and R. E. Kothmann. "Pressurized Solid Oxide Fuel Cell/Gas Turbine Power System." Contract # DE-AC26-98FT40355. Department of Energy, Pittsburgh, PA. February 2000.
8. Moran, Michael J. and Shapiro Howard N. *Fundamentals of Engineering Thermodynamics* 3rd ed. John Wiley & Sons, Inc., New York, 1996.
9. Scott, T.C., and R.E. Sonntag. University of Michigan, unpublished 1971, excerpt C₂H₆, C₃H₈, and C₄H₁₀ from K.A. Kobe, *Petroleum Refiner*, 28, No. 2. (1949).

10. Selection Process Technology, Department of Mechanical Engineering, Technische Universiteit Eindhoven.

http://www.wtb.tue.nl/woc/ptc/index.html?main=wissel/index.html?menu=menu_research.html

Appendix

Appendix A—Fortran Computer Model

Appendix B—Fortran Results

Appendix C—Economic Data

Appendix A

Fuel Cell Code written by Dr Krane:

```
*****
!
!
!           HYBRID MARK 2.f90
!
! *****
!
! BUILD: 1,2,3,4
! *****
!
!           VERSION 2
!
! *****
!
! THIS CODE SIMULATES THE PERFORMANCE OF A HYBRID GAS TURBINE/
! SOLID OXIDE FUEL CELL POWER GENERATION SYSTEM. THE SYSTEM
EMPLOYS
! A SOLAR 20 GAS TURBINE AND SIEMENS-WESTINGHOUSE TUBULAR SOLID
! OXIDE FUEL CELLS. BOTH THE GAS TURBINE AND THE FUEL CELLS ARE
! FUELED BY NATURAL GAS, WHICH IS ASSUMED TO BE PURE METHANE (CH4).
!
! WRITTEN BY: DR. ROBERT J. KRANE (SPRING, 2002)
!
! *****
! *****
! *****
!
!           SUBROUTINE ESTM (SINGLE PRECISION VERSION)
!
! *****
!
! THIS SUBROUTINE CALCULATES THE VALUE OF X WHICH YIELDS Y = 0
! FOR A GIVEN FUNCTION Y = Y(X) USING LAGRANGES INTERPOLATION
! FORMULA FOR A FIRST-THROUGH-SEVENTH DEGREE INTERPOLATION OR
! EXTRAPOLATION.
!
! *****
!
```


! ARGUMENTS IN THE CALL STATEMENT

! IDL - A COUNTER WHICH INDICATES THE NUMBER OF
! TIMES THE SUBROUTINE HAS BEEN ENTERED IN A
! GIVEN LOOP (20 MAX). IDL MUST BE INITIALIZED
! AND RESET (IF REQUIRED) IN THE CALLING PROGRAM.

! IN - THE DESIRED DEGREE OF FIT (1-7). EXPERIENCE HAS
! SHOWN THAT A SECOND DEGREE FIT (IN = 2) WORKS
! WELL IN MANY APPLICATIONS.

! XT, YT - SUBSCRIPTED VARIABLES WHICH GIVE A TABLE OF X-Y
! VALUES IF THE CALCULATION DOES NOT CONVERGE. XT
! AND YT MUST BE DIMENSIONED IN THE MAIN PROGRAM
! BY A STATEMENT OF THE FORM :
! DIMENSION XT(20),YT(20)

! YV - THE VARIABLE TO BE DRIVEN TO ZERO.

! XV - THE VARIABLE WHOSE VALUE MUST BE DETERMINED SUCH
! THAT Y = 0. ESTM OUTPUTS A NEW VALUE OF XV ON
! EACH PASS.

! LUPNAM - A HOLLERITH WORD OF NOT MORE THAN SIX
! CHARACTERS WHICH IDENTIFIES THE PARTICULAR
! LOOP IN CASE OF FAILURE TO CONVERGE. LUPNAM
! MUST BE SPECIFIED IN A DATA STATEMENT IN THE
! CALLING PROGRAM. EX : DATA LUP2/6H NO. 2 / .

! *****

! SUBROUTINE ESTM(IDL, IN, XT, YT, YV, XV, LUPNAM)

! DIMENSION XT(20), YT(20)
! 2 IDL = IDL + 1
! IF(IDL - 20) 5, 5, 60
! 5 XT(IDL) = XV
! YT(IDL) = YV
! IF(IDL - 1) 10, 10, 20
! 10 XV = 1.04D0 * XV
! RETURN
! 20 SUM = 0.D0
! IF(IDL - (IN+1)) 30, 30, 40
! 30 IM = 1
! GO TO 50
! 40 IM = IDL - IN
! 50 DO 3 I=IM, IDL
! PROD = XT(I)

```

DO 12 J=IM, IDL
A = YT(I) - YT(J)
IF( A ) 11, 12, 11
11 B = ( - YT(J) ) / A
    PROD = PROD * B
12 CONTINUE
3 SUM = SUM + PROD
    XV = SUM
    RETURN
60 CONTINUE
! 60 WRITE(6,70) LUPNAM, (I, XT(I), YT(I), I=1,20 )
! 70 FORMAT(1H1, //24X, 20HITERATION FAILED IN A6, 1X, 4HLOOP//13X
! !, 52HTHE INDEPENDENT AND DEPENDENT VARIABLE TABLES FOLLOW//
! !/19X, 1H1, 3X, 2HXT, 18X, 2HYT//20(I20, 2D20.8/))
    RETURN
    END
!
! *****
! *****
! *****
!
! SPECIFICATION STATEMENTS
!
! DIMENSION X1(20), Y1(20), X2(20), Y2(20), X3(20), Y3(20), X8(20), &
! & Y8(20)
!
! DATA STATEMENTS
!
! -DATA LUP1/6 No 1/
!
! *****
!
! STATEMENT FUNCTIONS TO CALCULATE ENTHALPY CHANGES FOR
SUBSTANCES
! BEING MODELED AS IDEAL GASES WITH VARIABLE SPECIFIC HEATS
! (TEMPERATURES T1 AND T2 MUST BE IN K)
!
! OXYGEN
!
! DHO2(T1,T2)= 3743.2*((T2/100.)-(T1/100.))           &
! & + .8041*((T2/100.)**2.5 - (T1/100.)**2.5)         &
! & + 35714. *((T2/100.)**-.5 - (T1/100.)**-.5)       &
! & - 23688. *((T2/100.)**-1.0 - (T1/100.)**-1.0)
!
! NITROGEN
!

```

$$\begin{aligned} \text{DHN2}(T1,T2) &= 3906.*((T2/100.) - (T1/100.)) && \& \\ &\& + 102558.*((T2/100.)**-.5 - (T1/100.)**-.5) && \& \\ &\& - 107270.*((T2/100.)**-.10 - (T1/100.)**-.10) && \& \\ &\& + 41020.*((T2/100.)**-.20 - (T1/100.)**-.20) \end{aligned}$$

! METHANE

$$\begin{aligned} \text{DHCH4}(T1,T2) &= -67287.*((T2/100.) - (T1/100.)) && \& \\ &\& + 35179.2*((T2/100.)**1.25 - (T1/100.)**1.25) && \& \\ &\& - 1421.43*((T2/100.)**1.75 - (T1/100.)**1.75) && \& \\ &\& + 64776.*((T2/100.)**-.5 - (T1/100.)**-.5) \end{aligned}$$

! CARBON DIOXIDE

$$\begin{aligned} \text{DHCO2}(T1,T2) &= -373.57*((T2/100.) - (T1/100.)) && \& \\ &\& + 2035.27*((T2/100.)**1.5 - (T1/100.)**1.5) && \& \\ &\& - 205.17*((T2/100.)**2.0 - (T1/100.)**2.0) && \& \\ &\& + .81*((T2/100.)**3.0 - (T1/100.)**3.0) \end{aligned}$$

! WATER

$$\begin{aligned} \text{DHH2O}(T1,T2) &= 14305.*((T2/100.) - (T1/100.)) && \& \\ &\& - 14683.2*((T2/100.)**1.25 - (T1/100.)**1.25) && \& \\ &\& + 5516.73*((T2/100.)**1.5 - (T1/100.)**1.5) && \& \\ &\& - 184.945*((T2/100.)**2.0 - (T1/100.)**2.0) \end{aligned}$$

! HYDROGEN

$$\begin{aligned} \text{DHH2}(T1,T2) &= 5650.5*((T2/100.) - (T1/100.)) && \& \\ &\& - 281096.*((T2/100.)**-.25 - (T1/100.)**-.25) && \& \\ &\& + 116500.*\text{LOG}((T2/100.)/(T1/100.)) && \& \\ &\& + 112140.*((T2/100.)**-.5 - (T1/100.)**-.5) \end{aligned}$$

! LOAD DATA FOR THE GAS TURBINE MODEL

! COMPRESSOR PRESSURE RATIO (-)

! RC = 9.2 ! VALUE FOR SOLAR SATURN 20 GT

```

! COMPRESSOR INLET TEMPERATURE (IN K)
!
  T01 = 288.
!
! TURBINE INLET TEMPERATURE (IN K)
!
  T041 = 1161. ! VALUE FOR SOLAR SATURN 20 GT
!
! SUM OF NORMALIZED TOTAL PRESSURE LOSSES (DELP0/P0) (.04 - .07) (-)
!
  SUMDELPOP = .085 ! SELECTED BY TRIAL AND ERROR FOR THE SATURN
20
!
! INITIAL ESTIMATE OF MASS FLOWRATE OF AIR (IN LBM/S)
!
  EMA = 16.0 !VALUE FOR SOLAR SATURN 20 GT
!
! GENERATOR EFFICIENCY (97.5% - 98.5%, REF: FLETCHER & WALSH)
!
  ETAGEN = .97 ! SELECTED BY TRIAL AND ERROR FOR THE SATURN 20
!
! GEAR BOX EFFICIENCY (97.5% < ETAGB < 99%), (REF: W&F),(-)
!
  ETAGB = .975
!
! FACTOR TO ACCOUNT FOR MECHANICAL LOSSES AND "WINDAGE" (REF.:
K&W)
!
  EPSML = .02
!
! ELECTRICAL OUTPUT UNDER ISO CONDITIONS (KW)
!
  WDOTEL = 1. !VALUE FOR SOLAR SATURN 20 GT FROM THERMOFLOW
CODE
!
!
!
! *****
!
! LOAD DATA FOR THE FUEL CELL MODEL
!
! FUEL UTILIZATION FACTOR
!
  UF = .85
!
! CELL OPERATING VOLTAGE (IN VOLTS)
!
  VCELL = .6

```

```

!
! TOTAL POWER TO BE GENERATED BY FUEL CELLS IN PLANT (MW)
!
TOTPOWFC = 2.7515
!
! *****
!
! LOAD DATA FOR HEAT EXCHANGER MODEL
!
ENTU = 1.5
!
! CONSTANT PRESSURE SPECIFIC HEATS FOR SYSTEM EXHAUST GAS
COMPONENTS
! (APPROXIMATE VALUES)
!
CPCO2 = .846 !(KJ/KG-K)
!
CPH2O = 1.8723 !(KJ/KG-K)
!
CPO2 = .918 !(KJ/KG-K)
!
CPN2 = 1.039 !(KJ/KG-K)
!
!
! OVERALL HEAT TRANSFER COEFFICIENT (KJ/H-K-M**2)
!
U = 100.
!
!
! *****
!
! COMPRESSOR EFFICIENCY (POLYTROPIC TOTAL-TO-TOTAL)
! REF: KORAKIANITUS AND WILSON
!
ETACP = .91 - (RC-1.0)/300.
!
ETACP = .85 ! THIS VALUE WAS SELECTED FOR THE SOLAR SATURN 20
! GAS TURBINE BY TRIAL AND ERROR RATHER THAN USING
! A VALUE CALCULATED BY THE ABOVE CORRELATION
! (WHICH APPLIES TO MUCH LARGER AXIAL FLOW
! COMPRESSORS THAN THE SATURN 20 COMPRESSOR).
!
!
! ITERATIVE LOOP TO COMPUTE COMPRESSOR OUTLET TEMPERATURE
!
! NOTE: EXTENSIVE TESTING SHOWS THAT THE CONVERGENCE OF THIS
! LOOP IS ESSENTIALLY INDEPENDENT OF THE INITIAL ESTIMATE
!

```

```

! OF T02I. THIS IS TYPICAL OF THE ROBUST BEHAVIOR
! EXHIBITED BY SUBROUTINE ESTM.
!
! INITIALIZE COUNTER FOR USE IN SUBROUTINE ESTM
!
! IDUM = 0
!
! INITIAL ESTIMATE OF COMPRESSOR OUTLET TEMPERATURE
!
! T02I = T01 * RC**(8.314/(29.071*ETACP))
!
! AVERAGE MOLAR CONSTANT PRESSURE SPECIFIC HEAT OF AIR (KJ/KMOL-K)
!
! 1 CPAAVE = (DHO2(T01,T02I)+3.76*DHN2(T01,T02I))/((T02I - T01)*4.76)
!
! IMPROVED VALUE OF COMPRESSOR OUTLET TEMPERATURE
!
! T02 = T01* RC**(8.314/(CPAAVE*ETACP))
!
! DUMMY VARIABLE (WHOSE VALUE IS TO BE DRIVEN TO ZERO BY
! DETERMINING THE CORRECT VALUE FOR T02I)
!
! DUMMY = T02 - T02I
!
! IF(ABS(DUMMY) .GT.(.000001*T02)) THEN
!
! CALL ESTM(IDUM,2,X1,Y1,DUMMY,T02I,LUP1)
!
! GO TO 1
!
! END IF
!
!
!
! COMBUSTION CALCULATIONS
!
! HEATS OF FORMATION OF CO2, H2O, AND METHANE (IN KJ/KMOL)
!
! HF0CO2 = -393520.
!
! HF0H2O = -241820.
!
! HF0CH4 = -74850.
!
!
! RATIO OF MOLAR FLOWRATE OF OXYGEN AT COMPRESSOR INLET
! TO MOLAR FLOWRATE OF FUEL
!
!
!

```

```

PHI1 = HF0CO2 + DHCO2(298.,T041)           &
& + 2.0*(HF0H2O + DHH2O(298.,T041))       &
& - 2.0* DHO2(298.,T041)                   &
& - (HF0CH4 + DHCH4(298.,T01))

!
!
! ITERATIVE LOOP TO DETERMINE HEX COMPRESSOR AIR OUTLET
TEMPERATURE
!
! SET LOOP COUNTER FOR SUBROUTINE+ V ESTM
!
! IDUMT03 = 0
!
! INITIAL ESTIMATE OF COMPRESSOR AIR HEAT EXCHANGER OUTLET
! TEMPERATURE
!
! T03I = 1105.
!
90 PHI2 = DHO2(T041,T03I) + 3.76*DHN2(T041,T03I)
!
! RATIO OF MOLAR FLOWRATE OF O2 THROUGH COMPRESSOR TO MOLAR
! FLOWRATE OF FUEL (METHANE) USED BY THE GAS TURBINE
!
! ENO2ONF = PHI1/PHI2
!
!
!
! EXPANDER PRESSURE RATIO
!
! NOTE:
! SUMDELPOP IS ESSENTIALLY THE SUM OF THE NORMALIZED TOTAL
PRESSURE
! LOSSES IN THE COMBUSTOR AND THE FLOW PASSAGES CONNECTING THE
! COMPRESSOR TO THE COMBUSTOR AND THE COMBUSTOR TO THE
EXPANDER.
! KORAKIANITUS AND WILSON SUGGEST THAT (.04 < SUMDELPOP < .07).
!
! RE = RC*(1.0 - SUMDELPOP)
!
! EXPANDER EFFICIENCY (POLYTROPIC TOTAL-TO-TOTAL)
!
! ETAEP = .9 - (RE-1.)/250.
!
! ETAEP = .86 ! THIS VALUE WAS SELECTED FOR THE SOLAR SATURN 20
! GAS TURBINE BY TRIAL AND ERROR RATHER THAN USING
! A VALUE CALCULATED BY THE ABOVE CORRELATION
! (WHICH APPLIES TO MUCH LARGER AXIAL FLOW

```

```

!           EXPANDERS THAN THE SATURN 20 EXPANDER).
!
! ITERATIVE LOOP TO COMPUTE EXPANDER OUTLET TEMPERATURE
!
! NOTE: EXTENSIVE TESTING SHOWS THAT THE CONVERGENCE OF THIS
!       LOOP IS ESSENTIALLY INDEPENDENT OF THE INITIAL ESTIMATE
!       OF T02I. THIS IS TYPICAL OF THE ROBUST BEHAVIOR
!       EXHIBITED BY SUBROUTINE ESTM.
!
! INITIALIZE COUNTER FOR USE IN SUBROUTINE ESTM
!
! IDUME = 0
!
! INITIAL ESTIMATE OF EXPANDER OUTLET TEMPERATURE (IN K)
!
! T05I = 800.
!
! AVERAGE MOLAR CONSTANT PRESSURE SPECIFIC HEAT OF THE
COMBUSTION
! PRODUCTS IN THE EXPANDER (KJ/KMOL-K)
!
! 14 CPEAVE = (DHCO2(T05I,T041) + 2.*DHH2O(T05I,T041) +(ENO2ONF- 2.)*&
& DHO2(T05I,T041) + 3.76*ENO2ONF*DHN2(T05I,T041))/      &
& ( (1. + 4.76*ENO2ONF)*(T041 - T05I) )
!
! IMPROVED ESTIMATE OF EXPANDER OUTLET TEMPERATURE (IN K)
!
! T05 = T041 * (RE)** -((8.314*ETAEP)/CPEAVE)
!
! DUMMY VARIABLE (WHOSE VALUE IS TO BE DRIVEN TO ZERO BY
! DETERMINING THE CORRECT VALUE FOR T05)
!
! DUMMYE = T05 - T05I
!
! IF(ABS(DUMMYE) .GT. (.000001*T05)) THEN
!
! CALL ESTM(IDUME,2,X2,Y2,DUMMYE,T05I,LUP2)
!
! GO TO 14
!
! END IF
!
!
! RATIO OF MOLAR FLOWRATE OF AIR TO MOLAR FLOWRATE OF FUEL
!
! ENAONF = 4.76* ENO2ONF
!
! RATIO OF MASS FLOWRATE OF AIR TO MASS FLOWRATE OF FUEL

```



```

!
EMAOMF = (ENAONF*28.97)/16.04
!
!
! ITERATIVE LOOP TO COMPUTE THE MASS FLOWRATE OF AIR
!
! INITIALIZE COUNTER FOR USE IN SUBROUTINE ESTM
!
IDUMGEN = 0
!
! MASS FLOWRATE OF FUEL (IN LBM/S)
!
50 EMF = EMA/EMAOMF
!
! MOLAR FLOWRATE OF FUEL (IN KMOL/S)
!
ENF = EMF/(16.04 *2.2046)
!
! MOLAR FLOWRATE OF OXYGEN (THROUGH THE COMPRESSOR)
!
ENO2 = ENF*ENO2ONF
!
! COMPRESSOR POWER
!
WDOTC = ENO2*(DHO2(T01,T02) + 3.76*DHN2(T01,T02))
!
! EXPANDER POWER
!
WDOTE = ENF*(DHCO2(T05,T041) + 2.*DHH2O(T05,T041)      &
& + (ENO2ONF - 2.)* DHO2(T05,T041) +3.76*ENO2ONF*DHN2(T05,T041))
!
! GENERATOR OUTPUT (IN KW)
!
WGEN = ETAGEN*ETAGB*(1.0 - EPSML)*(WDOTE - WDOTC)
!
! ADJUST GAS TURBINE AIR MASS FLOWRATE TO OBTAIN SPECIFIED
! VALUE (WDOTEL) OF ELECTRICAL POWER GENERATED BY THE TURBINE
!
! DUMMY VARIABLE (WHOSE VALUE IS TO BE DRIVEN TO ZERO BY
! DETERMINING THE CORRECT VALUE FOR EMF)
!
DUMMYGEN = WGEN - WDOTEL
!
! IF(ABS(DUMMYGEN) .GT. (.000001*WDOTEL) ) THEN
!
CALL ESTM(IDUMGEN,2,X3,Y3,DUMMYGEN,EMA,LUP3)
!
GO TO 50

```

```

!
END IF
!
GAS TURBINE HEAT RATE
!
HR = (EMF*21597.*3600.)/WDOTEL
!
!
*****
*****
!
FUEL CELL MODEL
!
*****
!
THIS MODEL USES SIMPLIFIED PERFORMANCE CURVES BASED ON SIEMMENS-
! WESTINGHOUSE EXPERIMENTAL DATA FOR THEIR TUBULAR SOLID OXIDE
! FUEL CELL. THESE CELLS ARE CONFIGURED 24 TO THE STACK. THUS,
! CELLS MUST BE ADDED TO THE SYSTEM IN GROUPS OF 24.
!
*****
!
SYSTEM OPERATING PRESSURES (IN ATM)
!
P08 = 1./(1.-.01) !(IN ATM) -ACCOUNTS FOR MUFFLER & STACK LOSSES
!
P07 = P08/(1.-.01) !(IN ATM)-ACCOUNTS FOR DELP OF EX GAS IN HEX
!
P06 = P07/(1.-.01) !(IN ATM)- ACCOUNTS FOR DELP OF EX GAS IN SOFC
!
FUEL CELL OPERATING PRESSURE
!
CELLPRESS = (P06+P07)/2. !(IN ATM)
!
FUEL CELL DATA CURVE FITS (FOR V1 = .6 V AND V2 = .75 V)
!
EYE1 = 390. + 7.857*CELLPRESS
!
EYE2 = 180. + 7.143*CELLPRESS
!
CELL CURRENT (IN AMPS)
!
EYECCELL = EYE1 + ((EYE2-EYE1)/.15)*(VCELL - .6)
!
ACTUAL CELL POWER (IN WATTS)
!

```

PCELL = EYECCELL * VCELL
 !
 ! TOTAL NUMBER OF INDIVIDUAL FUEL CELLS TO BE REQUIRED (-)
 !
 ENCELL = (TOTPOWFC*10**6)/PCELL
 !
 ! TOTAL MOLAR FLOWRATE OF METHANE PER CELL (KMOL CH4/S)
 !
 ENCH4CELL = (186.554* EYECCELL)/((4.*UF)*(10**7)*3600.)
 !
 ! TOTAL MOLAR FLOWRATE OF METHANE FOR ALL FUEL CELLS (KMOL CH4/S)
 !
 ENCH4TOTAL = ENCELL*ENCH4CELL
 !
 ! MOLAR FLOWRATE OF OXIDIZER STREAM PER CELL (KMOL OX STR/S)
 !
 ENOXSTRCELL = (ENF*(1. + 4.76 * ENO2ONF)*3600.)/ENCELL
 !
 ! MOLAR FLOWRATE OF CO2 AT CELL INLET (KMOL CO2/S)
 !
 ENCO26 = ENF
 !
 ! MOLAR FLOWRATE OF WATER AT CELL INLET (KMOL/S)
 !
 ENH2O6 = 2.* ENF
 !
 ! MOLAR FLOWRATE OF OXYGEN AT CELL INLET (KMOL/S)
 !
 ENO26 = (ENO2ONF-2.)* ENF
 !
 ! MOLAR FLOWRATE OF NITROGEN AT CELL INLET (KMOL/S)
 !
 ENN26 = 3.76 * ENO2ONF * ENF
 !
 !
 !
 !
 ! MOLAR FLOWRATE OF CO2 AT CELL OUTLET (KMOL CO2/S)
 !
 ENCO27 = ENCO26 + ENCH4TOTAL
 !
 ! MOLAR FLOWRATE OF WATER AT CELL OUTLET (KMOL H2O/S)
 !
 ENH2O7 = ENH2O6 + 2.*ENCH4TOTAL
 !
 ! MOLAR FLOWRATE OF OXYGEN AT CELL OUTLET (KMOL O2/S)
 !
 ENO27 = ENO26 - 2.*ENCH4TOTAL

```

!
! MOLAR FLOWRATE OF NITROGEN AT CELL OUTLET (KMOL N2/S)
!
! ENN27 = ENN26
!
!
!
! ENERGY BALANCE ON ONE CELL
!
! INITIAL ESTIMATE OF OXIDIZER STREAM INLET TEMPERATURE (K)
!
! T06 = T05
!
! SET COUNTER FOR SUBROUTINE ESTM
!
! IDUM = 0
!
! COMPUTE TERMS IN ENERGY BALANCE EQUATION (EXHAUST GAS STREAM
! LEAVES CELL AT CELL OPERATING TEMPERATURE = 1273 K)
!
! 52 TERM1 = ENCH4CELL * HF0CH4
!
! TERM2 = ENCO26 * (HF0CO2 + DHCO2(298.,T06))
!
! TERM3 = ENH2O6 * (HF0H2O + DHH2O(298.,T06))
!
! TERM4 = ENO26 * DHO2(298.,T06)
!
! TERM5 = ENN26 * DHN2(298., T06)
!
! TERM6 = ENCO27 * (HF0CO2 + DHCO2(298.,1273.))
!
! TERM7 = ENH2O7 * (HF0H2O + DHH2O(298.,1273.))
!
! TERM8 = ENO27 * DHO2(298.,1273.)
!
! TERM9 = ENN27 * DHN2(298.,1273.)
!
! TERM10 = .001* PCELL
!
! DUMMY VARIABLE WHOSE VALUE IS TO BE DRIVEN TO ZERO BY
! DETERMINING
! THE CORRECT VALUE FOR T06
!
! BAL = (TERM1 + TERM2 + TERM3 + TERM4 + TERM5           &
!       & - TERM6 - TERM7 - TERM8 - TERM9 - TERM10 )
!

```

```

IF(ABS(BAL) .GT. 1.) THEN
!
CALL ESTM(IDUM,2,X8,Y8,BAL,T06,LUP8)
!
GO TO 52
!
ENDIF
!
!
!
! HEAT EXCHANGER MODEL (EPSILON-NTU MODEL)
!
! N.B. HEX IS A SINGLE-PASS CROSS-FLOW HEX WITH BOTH FLUIDS UNMIXED
!
! MASS FLOWRATES OF EXHAUST GAS COMPONENTS (THROUGH HEX,
MUFFLER,
! AND STACK)
!
EMCO2EX = 44.* ENCO27  ! (MASS FLOWRATE OF CO2 - IN KG/S)
!
EMH2OEX = 18.* ENH2O7  ! (MASS FLOWRATE OF H2O - IN KG/S)
!
EMO2EX = 32.* ENO27    ! (MASS FLOWRATE OF O2 - IN KG/S)
!
EMN2EX = 28.* ENN27    ! (MASS FLOWRATE OF N2 - IN KG/S)
!
! TOTAL MASS FLOWRATE OF SYSTEM EXHAUST GAS ( IN KG/S )
!
EMEXGAS = EMCO2EX + EMH2OEX + EMO2EX + EMN2EX
!
! CONSTANT PRESSURE SPECIFIC HEAT OF EXHAUST GAS (APPROIMATE: USES
! CONSTANT VALUES OF COMPONENT GAS CP'S) - IN (KJ/KG-K)
!
CPEXGAS = (EMCO2EX*CPCO2)/EMEXGAS + (EMH2OEX*CPH2O)/EMEXGAS  &
& + (EMO2EX*CPO2)/EMEXGAS + (EMN2EX*CPN2)/EMEXGAS
!
! THERMAL CAPACITY RATE OF EXHAUST GAS (HOT) STREAM IN (KJ/S-K)
!
CH = EMEXGAS*CPEXGAS
!
!
! MASS FLOWRATE OF O2 THROUGH COMPRESSOR (IN KG/S)
!
EMO2COMP = 32.*ENO2ONF*ENF
!
! MASS FLOWRATE OF N2 THROUGH COMPRESSOR (IN KG/S)
!

```

```

EMN2COMP = 28.*3.76*ENO2ONF*ENF
!
! MASS FLOWRATE OF COMPRESSOR AIR (IN KG/S)
!
EMCOMPAIOLD = EMO2COMP + EMN2COMP  !(FOR CHECK ON CELL MASS
BALANCE)
!
EMCOMPAIR = EMA/2.2046
!
! THERMAL CAPACITY RATE OF COMPRESSOR (COLD) STREAM (IN KJ/H-K)
!
CC = EMCOMPAIR*1.005
!
! MINIMUM THERMAL CAPACITY RATE FOR THE HEX
!
CMIN = MIN(CH,CC)
!
! MAXIMUM THERMAL CAPACITY RATE FOR THE HEX
!
CMAX = MAX(CH,CC)
!
! THERMAL CAPACITY RATE RATIO FOR THE HEX (-)
!
CRAT = CMIN/CMAX
!
! ARGUMENT FOR THE EFFECTIVENESS (EPSILON) EXPRESSION (-)
!
ARG1 = (EXP(-CRAT*ENTU**.78)-1.)*(ENTU**.22)/CRAT
!
! HEAT EXCHANGER EFFECTIVENESS (-)
!
EPSILON = 1. - EXP(ARG1)
!
! OUTLET TEMPERATURE OF THE EXHAUST GAS (HOT) STREAM (IN K)
!
T08 = 1273. - EPSILON*CMIN*(1273.-T02)/CH
!
! OUTLET TEMPERATURE OF THE COMPRESSOR AIR (COLD) STREAM (IN K)
!
T03 = T02 + (CH/CC)*(1273. - T08)
!
! CHECK FOR CONVERGENCE OF T03 (COMPR. AIR HEX OUTLET TEMP)
!
TDUMMY = T03 - T03I
!
IF(ABS(TDUMMY) .GT. (.000001*T03I)) THEN
!
CALL ESTM(IDUMT03,2,X2,Y2,TDUMMY,T03I,LUP50)

```

```

!
GO TO 90
!
ENDIF
!
ESTIMATE OF HEAT EXCHANGER AREA (IN M**2)
!
AHEX = (CMIN*ENTU*3600.)/U      ! U IN (KJ/H-K-M**2)
!
RATE OF HEAT TRANSFER TO COLD STREAM (IN KJ/H)
!
QHEX = CH*(1273.-T08)
!
CHECK VALUE FOR QHEX
!
QHEXCHECK = CC*(T03-T02)
!
!
FUEL CELL PREHEATER
!
THIS PREHEATER IS A SMALL FIRED HEAT EXCHANGER IN WHICH
! THE GAS TURBINE EXHAUST IS HEATED UP TO THE REQUIRED FUEL
! CELL INLET TEMPERATURE (T06) BY THE COMBUSTION OF METHANE.
! FOR SIMPLICITY, IT IS ASSUMED THAT THE METHANE IS BURNT WITH
! AIR AND THE EXHAUST PRODUCTS ARE NOT ADDED TO THOSE OF THE GAS
! TURBINE EXHAUST. ONLY THE HEAT FROM THIS COMBUSTION IS
! TRANSFERRED TO THE GAS TURBINE EXHAUST STREAM. ANY METHANE
USED
! IN THE PREHEATER MUST BE ADDED TO THE AMOUNTS USED BY THE GAS
! TURBINE AND THE FUEL CELLS.
!
RATE OF HEAT TRANSFER IN PREHEATER (IN KMOL/S)
!
QPH = ENCO26*DHCO2(T05,T06) + ENH2O6*DHH2O(T05,T06)      &
      & + ENO26*DHO2(T05,T06) + ENN26*DHN2(T05,T06)
!
MOLAR FLOWRATE OF METHANE FOR THE PREHEATER (KMOL/S)
!
ENCH4PH = QPH/241878.  ! (241878 KJ/KMOL = LHV OF METHANE )
!
OUTPUT STATEMENTS
!
      WRITE(*,3) DUMMY
3 FORMAT(3X,'DUMMY = ',E14.7)
!
      WRITE(*,4) CPAAVE
4 FORMAT(3X,'CPAAVE = ',E14.7)

```

```

!
    WRITE(*,7) IDUM
7 FORMAT(3X,'IDUM = ',I3)
!
    WRITE(*,8) PHI1
8 FORMAT(3X,'PHI1 = ', E14.7)
!
    WRITE(*,9) PHI2
9 FORMAT(3X,'PHI2 = ', E14.7)
!
    WRITE(*,10) ENO2ONF
10 FORMAT(3X,'ENO2ONF = ', E14.7)
!
    WRITE(*,6) RE
6 FORMAT(3X,'RE = ', E14.7)
!
    WRITE(*,51) ETACP
51 FORMAT(3X,'ETACP = ', E14.7)
!
    WRITE(*,11) ETAEP
11 FORMAT(3X,'ETAEP = ', E14.7)
!
    WRITE(*,16) CPEAVE
16 FORMAT(3X,'CPEAVE = ',E14.7)
!
    WRITE(*,15) IDUME
15 FORMAT(3X,'IDUME =',I3)
!
    WRITE(*,17) ETACP
17 FORMAT(3X,'ETACP =',E14.7)
!
    WRITE(*,18) DUMMYE
18 FORMAT(3X,'DUMMYE = ',E14.7)
!
    WRITE(*,24) ENAONF
24 FORMAT(3X,'ENAONF = ',E14.7)
!
!
    WRITE(*,20)EMAOMF
20 FORMAT(3X,'EMAOMF = ',E14.7)
!
    WRITE(*,21) EMF
21 FORMAT(3X,'EMF = ',E14.7)
!
    WRITE(*,22)HR
22 FORMAT(3X,'HR = ',E14.7)
!
    WRITE(*,26)ENF

```



```

26 FORMAT(3X,'ENF = ',E14.7)
!
  WRITE(*,27)ENO2
27 FORMAT(3X,'ENO2 = ',E14.7)
!
  WRITE(*,28)WDOTC
28 FORMAT(3X,'WDOTC = ',E14.7)
!
  WRITE(*,29)WDOTE
29 FORMAT(3X,'WDOTE = ',E14.7)
!
  WRITE(*,30)EMA
30 FORMAT(3X,'EMA = ',E14.7)
!
  WRITE(*,23)WGEN
23 FORMAT(3X,'WGEN = ',E14.7)
!
  WRITE(*,40)DUMMYGEN
40 FORMAT(3X,'DUMMYGEN = ',E14.7)
!
  WRITE(*,41)IDUMGEN
41 FORMAT(3X,'IDUMGEN = ',E14.7)
!
  WRITE(*,44)BAL
44 FORMAT(3X,'BAL = ',E14.7,/)
!
  WRITE(*,54)UF
54 FORMAT(3X,'UF = ',E14.7)
!
  WRITE(*,56)VCELL
56 FORMAT(3X,'VCELL = ',E14.7)
!
  WRITE(*,57)TOTPOWFC
57 FORMAT(3X,'TOTPOWFC = ',E14.7)
!
  WRITE(*,59)P06
59 FORMAT(3X,'P06 = ',E14.7)
!
  WRITE(*,60)P07
60 FORMAT(3X,'P07 = ',E14.7)
!
  WRITE(*,61)P08
61 FORMAT(3X,'P08 = ',E14.7)
!
  WRITE(*,62)CELLPRESS
62 FORMAT(3X,'CELLPRESS = ',E14.7)
!
  WRITE(*,63)EYECCELL

```

```

63 FORMAT(3X,'EYECCELL = ',E14.7)
!
  WRITE(*,64)PCELL
64 FORMAT(3X,'PCELL = ',E14.7)
!
  WRITE(*,65)ENCELL
65 FORMAT(3X,'ENCELL = ',E14.7)
!
  WRITE(*,66) ENCH4CELL
66 FORMAT(3X, 'ENCH4CELL = ',E14.7)
!
  WRITE(*,67)ENCH4TOTAL
67 FORMAT(3X,'ENCH4TOTAL = ',E14.7,/)
!
  WRITE(*,2) T02
    2 FORMAT(3X,'T02 = ',E14.7)
!
  WRITE(*,68) T03
68 FORMAT(3X,'T03 = ',E14.7)
!
  WRITE(*,12) T05
12 FORMAT(3X,'T05 = ', E14.7)
!
  WRITE(*,69) T06
69 FORMAT(3X,'T06 = ',E14.7)
!
  WRITE(*,70)
70 FORMAT(3X,'T07 = 1273.')
```



```

  WRITE(*,71) T08
71 FORMAT(3X,'T08 = ',E14.7,/)
!

  WRITE(*,55)U
55 FORMAT(3X,'U = ',E14.7)
!
  WRITE(*,58)ENTU
58 FORMAT(3X,'ENTU = ',E14.7)
!
  WRITE(*,73) CH
73 FORMAT(3X,'CH = ', E14.7)
!
  WRITE(*,74) CC
74 FORMAT(3X,'CC = ', E14.7)
  WRITE(*,76) CMIN
76 FORMAT(3X,'CMIN = ', E14.7)
!
  WRITE(*,77) CMAX
```

```

77 FORMAT(3X,'CMAX = ', E14.7)
!
WRITE(*,78) EPSILON
78 FORMAT(3X,'EPSILON = ', E14.7)
!
WRITE(*,79) AHEX
79 FORMAT(3X,'AHEX = ', E14.7)
!
WRITE(*,80) QHEX
80 FORMAT(3X,'QHEX = ', E14.7)
!
WRITE(*,81) QHEXCHECK
81 FORMAT(3X,'QHEXCHECK = ', E14.7,/)
!
WRITE(*,100)QPH
100 FORMAT(3X,'QPH = ',E14.7)
!
WRITE(*,101)ENCH4PH
101 FORMAT(3X,'ENCH4PH = ',E14.7,/)
!
WRITE(*,75) EMCOMPAIR
75 FORMAT(3X,'EMCOMPAIR = ', E14.7)
!
WRITE(*,83) CPEXGAS
83 FORMAT(3X, 'CPEXGAS =',E14.7)
!
!
!
WRITE(*,82) TDUMMY
82 FORMAT(3X, 'TDUMMY =',E14.7)
!
WRITE(*,84)EMCO2EX
84 FORMAT(3X, 'EMCO2EX =',E14.7)
!
WRITE(*,85)EMH2OEX
85 FORMAT(3X,'EMH2OEX = ',E14.7)
!
WRITE(*,86)EMO2EX
86 FORMAT(3X,'EMO2EX = ',E14.7)
!
WRITE(*,87)EMN2EX
87 FORMAT(3X,'EMN2EX = ',E14.7)
!
WRITE(*,72) EMEXGAS
72 FORMAT(3X,'EMEXGAS = ',E14.7)
!
!
END

```

Appendix B

DUMMY = -0.6103516E-04
CPAAVE = 0.2968115E+02
IDUM = 3
PHI1 = -0.7507636E+06
PHI2 = -0.2881119E+05
ENO2ONF = 0.2605806E+02
RE = 0.8418000E+01
ETACP = 0.8500000E+00
ETAEP = 0.8600000E+00
CPEAVE = 0.3310723E+02
IDUME = 3
ETACP = 0.8500000E+00
DUMMYE = 0.0000000E+00
ENAONF = 0.1240364E+03
EMAOMF = 0.2240233E+03
EMF = 0.9866294E-01
HR = 0.4711895E+04
ENF = 0.2790101E-02
ENO2 = 0.7270461E-01
WDOTC = 0.3188519E+04
WDOTE = 0.4945034E+04
EMA = 0.2210279E+02
WGEN = 0.1628000E+04
DUMMYGEN = -0.2441406E-03
IDUMGEN = 0.2802597E-44
BAL = -0.1042005E-02
UF = 0.8500000E+00
VCELL = 0.6000000E+00
TOTPOWFC = 0.2751500E+01
P06 = 0.1030610E+01
P07 = 0.1020304E+01
P08 = 0.1010101E+01
CELLPRESS = 0.1025457E+01
EYECCELL = 0.3980570E+03
PCCELL = 0.2388342E+03
ENCELL = 0.1152054E+05
ENCH4CELL = 0.6066922E-06
ENCH4TOTAL = 0.6989424E-02
T02 = 0.5984127E+03
T03 = 0.9804462E+03
T05 = 0.7328556E+03
T06 = 0.7845570E+03
T07 = 1273.
T08 = 0.9076938E+03
U = 0.1000000E+03
ENTU = 0.1500000E+01
CH = 0.1053726E+02
CC = 0.1007589E+02
CMIN = 0.1007589E+02
CMAX = 0.1053726E+02
EPSILON = 0.5663218E+00
AHEX = 0.5440981E+03
QHEX = 0.3849328E+04
QHEXCHECK = 0.3849328E+04
QPH = 0.5764183E+03
ENCH4PH = 0.7185828E-03
EMCOMPAIR = 0.1002576E+02
CPEXGAS = 0.1039448E+01
TDUMMY = 0.5493164E-03
EMCO2EX = 0.4302990E+00
EMH2OEX = 0.3520629E+00
EMO2EX = 0.1700658E+01
EMN2EX = 0.7654342E+01
EMEXGAS = 0.1013736E+02

Appendix C

Table C1: Siemens 19MW hybrid power plant installed capital cost summary

Installed Equipment Costs					
	Equipment	Freight	Installation	Totals	
SOFC Generator	\$8,890,422	\$31,500	\$47,365	\$8,969,287	
Gas Turbine System	3,960,682	3,500	59,347	4,023,529	
SOFC Power Conditioning System	1,988,520	15,750	24,374	2,028,644	
Instrumentation, Controls, and Electrical Cabinets	877,542	7,000	199,520	1,084,062	
Switchyard and Electrical Distribution	959,600		237,980	1,197,580	
Fuel Supply System	167,091	1,750	10,000	178,841	
Hydrogen Supply System	89,779	1,750	10,000	101,529	
Purge Gas Supply System	120,520	1,750	10,000	132,270	
Auxiliary Air Supply System	179,723	1,750	6,510	187,983	
Startup Boiler System	74,884	1,750	1,316	77,950	
Piping and Insulation	1,608,054	15,750	317,649	1,941,453	
Site Buildings				36,159	
Totals	\$18,916,817	\$82,250	\$924,061	\$19,959,287	
Project Cost Summary					
Installed Equipment					\$19,959,287
Project Management, Engineering, and Permitting					919,369
Site Preparation					412,994
Grading, utilities installation				\$145,744	
Foundations installation				217,519	
Structural steel installation				49,731	
G&A, R&D, Sales & Marketing, Profit Allowance					5,544,303
Total Plant Cost					\$26,835,953
Spare Parts Allowance					246,914
Startup					150,000
Land					20,000
Total Capital Requirement					\$27,252,867

Table C2: Present worth study broken down by year

Year	0	1	2	3	4	5	6
Gross Cash Flow for Year	-4869037.314	1217469.001	1217469.001	1217469.001	1217469.001	1217469.001	1217469.001
Depreciation Expense	0	243451.8657	243451.8657	243451.8657	243451.8657	243451.8657	243451.8657
Income prior to taxes	-4869037.314	974017.1352	974017.1352	974017.1352	974017.1352	974017.1352	974017.1352
Income tax expense	-1460711.194	292205.1406	292205.1406	292205.1406	292205.1406	292205.1406	292205.1406
Income after taxes	-3408326.12	681811.9946	681811.9946	681811.9946	681811.9946	681811.9946	681811.9946
Net income for year	-3408326.12	925263.8603	925263.8603	925263.8603	925263.8603	925263.8603	925263.8603
Present Worth	-3408326.12	797641.2589	687621.7749	592777.3922	511014.9932	440530.1666	379767.385

Year	7	8	9	10	11	12	13
Gross Cash Flow for Year	1217469.001	1217469.001	1217469.001	1217469.001	1217469.001	1217469.001	1217469.001
Depreciation Expense	243451.8657	243451.8657	243451.8657	243451.8657	243451.8657	243451.8657	243451.8657
Income prior to taxes	974017.1352	974017.1352	974017.1352	974017.1352	974017.1352	974017.1352	974017.1352
Income tax expense	292205.1406	292205.1406	292205.1406	292205.1406	292205.1406	292205.1406	292205.1406
Income after taxes	681811.9946	681811.9946	681811.9946	681811.9946	681811.9946	681811.9946	681811.9946
Net income for year	925263.8603	925263.8603	925263.8603	925263.8603	925263.8603	925263.8603	925263.8603
Present Worth	327385.6767	282229.0317	243300.8894	209742.146	180812.1948	155872.5817	134372.9153

Year	14	15	16	17	18	19	20
Gross Cash Flow for Year	1217469.001	1217469.001	1217469.001	1217469.001	1217469.001	1217469.001	1217469.001
Depreciation Expense	243451.8657	243451.8657	243451.8657	243451.8657	243451.8657	243451.8657	243451.8657
Income prior to taxes	974017.1352	974017.1352	974017.1352	974017.1352	974017.1352	974017.1352	974017.1352
Income tax expense	292205.1406	292205.1406	292205.1406	292205.1406	292205.1406	292205.1406	292205.1406
Income after taxes	681811.9946	681811.9946	681811.9946	681811.9946	681811.9946	681811.9946	681811.9946
Net income for year	925263.8603	925263.8603	925263.8603	925263.8603	925263.8603	925263.8603	925263.8603
Present Worth	115838.7201	99860.96559	86087.0393	74212.96492	63976.69389	55152.32232	47545.10545

Year	21	22	23	24	25	26	27
Gross Cash Flow for Year	1217469.001	1217469.001	1217469.001	1217469.001	1217469.001	1217469.001	1217469.001
Depreciation Expense	0	0	0	0	0	0	0
Income prior to taxes	1217469.001	1217469.001	1217469.001	1217469.001	1217469.001	1217469.001	1217469.001
Income tax expense	365240.7003	365240.7003	365240.7003	365240.7003	365240.7003	365240.7003	365240.7003
Income after taxes	852228.3006	852228.3006	852228.3006	852228.3006	852228.3006	852228.3006	852228.3006
Net income for year	852228.3006	852228.3006	852228.3006	852228.3006	852228.3006	852228.3006	852228.3006
Present Worth	37751.84475	32544.69375	28055.77047	24186.00903	20850.00778	17974.14464	15494.95228

Year	28	29	30
Gross Cash Flow for Year	1217469.001	1217469.001	1217469.001
Depreciation Expense	0	0	0
Income prior to taxes	1217469.001	1217469.001	1217469.001
Income tax expense	365240.7003	365240.7003	365240.7003
Income after taxes	852228.3006	852228.3006	852228.3006
Net income for year	852228.3006	852228.3006	852228.3006
Present Worth	13357.71748	11515.27369	9926.960076

Total present worth of project =	2289073.472
---	--------------------